AN INTEGRATED GEOPHYSICAL STUDY OF THE NEMAHA UPLIFT/HUMBOLDT FAULT ZONE, WABAUNSEE AND RILEY COUNTIES, KANSAS

by

Nathan Allan Geier

Kansas Geological Survey
Open-file Report 99-35

An Integrated Geophysical Study of the Nemaha Uplift/Humboldt Fault Zone, Wabaunsee and Riley Counties, Kansas

by

Nathan Allan Geier
B.S., Kansas State University, 1997

Submitted to the Department of Geology and the Faculty of the Graduate School of the University of Kansas in partial fulfillment of the requirements for the degree of Master of Science.

Advisory Committee:

_____
Chair

_____

_____

_____
Committee Members

_____
For the Department

_____
Date Thesis Accepted

Abstract

The Humboldt Fault zone defines the eastern edge of the Nemaha uplift. The Humboldt Fault zone/Nemaha uplift system is the most structurally complex geologic feature of Kansas. This northeast-trending, regionally linear feature can be traced across the entire state. Seismic and drill data suggest a complex set of high-angle reverse and normal faults that posses over 600 m of cumulative displacement of the Precambrian granitic basement. In northeastern Kansas, the uplift separates the Salina basin – Forest City basin.

An integrated geophysical survey was conducted in northern Wabaunsee and southern Riley counties, Kansas to gain a better understanding of the structural nature and geological history of the Humboldt Fault zone/Nemaha uplift system. A high resolution seismic profile, a magnetic profile, and gravity profile traversed the uplifts and bounding fault zones.

Seismic data defined two major phases of faulting on the Humboldt Fault zone. A compressional stress regime resulted in high angle reverse faults with large offset (up to 300 m on a single fault) in Late Devonian – Early Pennsylvanian time. Smaller-scale (<50 m) normal faulting occurred after deposition of the Shawnee group (Virgilian stage) requiring either a shift to an extensional stress regime or relaxation of the previous compressional stress environment. A reversal in fault movement from reverse in pre-Pennsylvanian sedimentary rocks to normal faulting in Pennsylvanian aged sedimentary rocks suggests most normal faults occurred along pre-existing joints or small-scale reverse faults that formed during the compressional phase.

Eleven kilometers west of the Humboldt Fault zone and bounding the western edge of the Nemaha uplift is the newly interpreted Zeandale Fault zone. Cumulative offset across this fault zone is in excess of 300 m. Two episodes of faulting are interpreted that appear to coincide with the two phases of faulting interpreted on the Humboldt Fault zone. All faulting in this fault zone is interpreted to be normal, however. Based on drill, seismic, magnetic, and gravity data, the Zeandale Fault zone is a localized feature roughly 15 km in total length and subparallel to the Humboldt Fault zone.

Acknowledgements

I would sincerely like to thank the Chair of my committee, Rick Miller, and the Kansas Geological Survey for providing all of the funding necessary for the collection and processing of the presented data. I also thank Rick for his detailed criticisms of the interpretations of this data. I wish to express my gratitude to Drs. Don Steeples and Doug Walker for their guidance and insightful criticisms that helped to strengthen and focus this body of work.

Special thanks go out to Dr. Jianghia Xia who spent an inordinate amount of time providing software support, offering guidance of data processing, helping with the collection of the potential field data and the seismic data, and carrying on lengthy discussions with me about my research.

This research would not have been possible were it not for the time and effort of several Kansas Geological Survey staff members. Drs. Pieter Berendsen and John Doveton offered many suggestions throughout the course of this study. The Kansas Geological Survey seismic field crew spent a good portion of the summer of 1997 collecting this data. The field crew included: Rick Miller, David Laflin, Jianghai Xia, John Siceloff, Marina Feroci, Julian Ivanov, and Josh Steinlage. Brett Bennett provided hardware and software support throughout the course of this study. Julian Ivanov spent many hours with me discussing the mechanics of seismic processing in general as well as with the software used to process the seismic data.

I thank my parents, Alan and Nikki, for nurturing my love of the natural sciences for as long as I can remember, taking me to every natural history museum we came across, instilling in me the value of hard work and education, and for always believing in me.

Finally I would like to thank my wife, Katie, for offering her love, support, and understanding throughout the course of my graduate studies. I could not have completed this work without her.

Table of Contents

List of Figures

List of Tables

List of Plates

1. Introduction

To better understand the structure and geological history of the Humboldt Fault zone / Nemaha uplift system, several geophysical surveys were conducted in northern Wabaunsee and southern Riley counties, Kansas. The surveys traversed the Humboldt Fault zone and the Nemaha uplift at nearly right angles as determined by drill holes the encounter Precambrian basement. Three imaging methods were utilized:

1) Near Surface Seismic Profile
2) Gravity Profile
3) Magnetic Profile

Each data set was acquired along the same profile with parameters designed to compliment each other as closely as possible.

The Nemaha uplift is a 500 km long, N20E-trending, structural feature that stretches from southeastern Nebraska to just north of Oklahoma City, OK (Fig. 1.1). It extends across Kansas from Nemaha County in the north, to Sumner County in the south. The structure has only limited surface expression but dramatic presence in the subsurface. At the crest of the uplift, Precambrian basement is as shallow as 250 m at the Kansas-Nebraska border increasing to 1400 m at the Kansas-Oklahoma border. The uplift also narrows to the south, from as wide as 50 km in northeastern Kansas down to 3 km near the Oklahoma border (Fig. 1.1).

The Humboldt fault zone marks the eastern edge of the Nemaha uplift. Though originally interpreted as one long discontinuous normal fault (e.g. Cole, 1976), recent geologic and geophysical studies have suggested that it is really a zone of faults (e.g., Dubois, 1978; Steeples et al., 1979; Steeples, 1982) with compound offsets totalling as much as 800m (Berendsen and Blair,1995). If a wrench environment were present during Mississippian and Pennsylvanian time in association with the Ouachita Orogeny, it is reasonable to interpret a series of NE and NW trending anastomizing faults along the uplift (Berendsen and Blair, 1986; Berendsen and Blair, 1996). No physical evidence currently exists that supports this interpretation.

Interpretations presented in this paper are based on the three geophysical data sets as well as drill data, published geologic reports, and personal communications. The profile under study by this paper intersects as eight interpreted faults (Berendsen and Blair, 1996), with control provided by 8 boreholes that penetrate Precambrian basement within 2 miles of the 2-D cross-section. Imaging multiple faults, this study may offer direct support of the wrench environment interpretation of the Humboldt fault zone. The nature and location of all the faults along this profile have been better defined with the previous uniform block fault interpretations significantly enhanced.

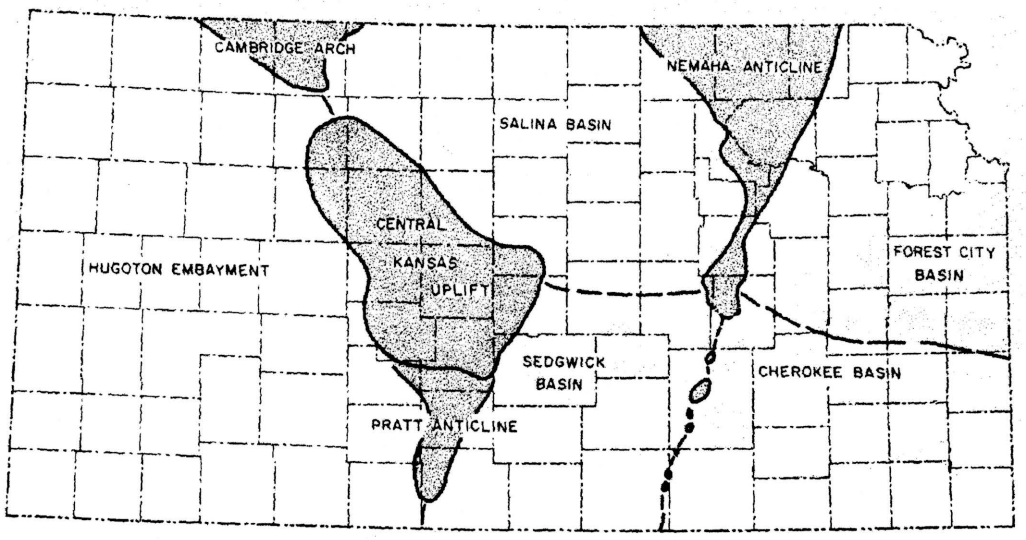

Figure 1.1 Map showing major structural features of Kansas. Of major concern to this study is the Nemaha uplift. (Modified from, Merriam, 1963)

2. Background

To fully understand the significance of this study it is important to review the regional stratigraphy and chronological sequence of events in the region. Complimenting this review will be a look at previous geophysical studies in the region of the Nemaha uplift/Humboldt Fault zone.

2.1 Geology

The Humboldt Fault zone bounds the eastern edge of the Nemaha uplift, and both combine to represent one of the most significant structural features in Kansas. This significance relates to the role it plays bounding the western edge of the Forest City basin and the Cherokee basin, and the eastern edge of the Salina basin and the Sedgwick basin. The Nemaha uplift is a geographically extensive feature traceable across the entire state of Kansas, from Nemaha County, KS in the north, to Sumner County, KS in the south. The uplift is regionally a linear feature trending N20E across the state (Fig. 1.1).

In the area of this study, the Nemaha uplift separates the Salina and Forest City basins, making the generalized stratigraphy of these two basins relevant to this study. Understanding the timing of the Nemaha uplift, especially as it relates to Paleozoic displacement on the Humboldt fault, is key to appreciating the temporal development of the two basins as well as the structure of the interbasinal area.

2.1.1 Generalized Stratigraphy and Major Unconformities

The thickness of the Paleozoic section varies dramatically along the profile studied. The Forest City basin is imaged under the first 7 km on the east end of the profile where the Paleozoic section is essentially 900 m (3000 ft) thick (Cole and Watney, 1985). Several miles to the west, at the crest of the Nemaha uplift and in the middle of the profile, the Paleozoic section is as thin as 300 m (1000 ft) (Cole and Watney, 1985). This several hundred-meter change in depth to basement occurs over 10 km based on drill data. Thinning of the Paleozoic section resulted from erosion or non-deposition of units along the crest of the uplift, which was a positive feature at the time of deposition. The western end of the profile is within the Salina basin. Based on drill data, thickness of the Paleozoic section at this end of the profile is around 600 m (2000 ft).

It should be noted that 25 km further to the west the tops of the Precambrian rocks switch from granite to a mixed assemblage of sandstone and volcanics named the Rice formation deposited in a rift environment (Berendsen and Blair, 1996) and are estimated to be 1100 Ma to 535 Ma in age (Berendsen, 1994). Roughly 40 km to the west a suite of mafic intrusives and extrusives (Berendsen and Blair, 1996) characterizes the Precambrian surface. These rocks are postulated to represent the remnants of a failed rift. The age of these mafic rocks, and thus the rift, is 1100 Ma.

Paleozoic rocks along the profile of the study are sedimentary. Most are shallow marine in nature, primarily carbonates and shales, with some intermittent sandstones (Zeller, 1968; Baars and Maples, 1995).

The Precambrian surface is a major unconformity. Along the profile, all of the wells to the Precambrian have yielded granitic rock (Cole and Watney, 1985) 1.45-1.7 billion years in age (Bickford and others, 1979). Basinward, this unconformity marks 600 m.y. of missing sedimentary rocks, while at the crest of the uplift, as much as 800 m.y. of stratigraphic section cannot be accounted for (Berendsen, 1996). The first major unit overlying the Precambrian unconformity in this area is a Cambro-Ordovician dolomitic limestone of the Arbuckle Group. Another major unconformity is present at the top of the Arbuckle. This unconformity is early to middle Ordovician in age and is regionally extensive. On top of this unconformity is the middle Ordovician Simpson group consisting primarily of sandstone grading upwards into a shale. Lying on top of the Simpson is the Viola limestone (Middle Ordovician), the Maquoketa shale (upper Ordovician), and the dolomitic limestone dominated Hunton Group (Silurian-Devonian). A regional extensive unconformity defines the boundary between Silurian and the Devonian (Steeples, 1989).

Major uplift occurred along the Nemaha anticline during the Mississippian. This uplift is consistent with a major unconformity in the Salina and Forest City basins. A major discrepancy exits between the two basin's Mississippian sediment packages. In the Forest City basin, Mississippian aged sediments are roughly 120 m in total thickness. However, Mississippian rocks are absent in the Salina basin (Merriam, 1963). Along the axis of the Nemaha uplift, Pennsylvanian units lie in direct contact with the Precambrian basement. The Lansing and Kansas City groups (Pennsylvanian) are a contiguous series of interbedded sandstones, limestones, and shales. Surface rocks along the profile range in age from Pennsylvanian to Permian, with Pennsylvanian aged bedrock in the Forest City basin and Permian aged bedrock in the Salina basin and across the Nemaha uplift. With no post-Permian sedimentary rocks present, the geological record of the last 245 m.y. has been lost or obscured.

2.1.2 Structure and Timing of Events

A major geologic feature and geophysical anomaly (MGA) of the mid-continent is a 1.1 Ga failed rift which runs from Lake Superior south-westward into north-central Kansas (Fig. 2.1). The feature possess a pronounced gravity and magnetic signature and has been well documented over the last 50 years (e.g. Wollard, 1943; Lyons, 1959). The Nemaha uplift lies on the eastern flank of the rift zone, with the Humboldt Fault zone making up an integral part of the Mid-continent rift system (Berendsen and Blair, 1995). Early reports (e.g. Lee, 1956; Merriam, 1963)

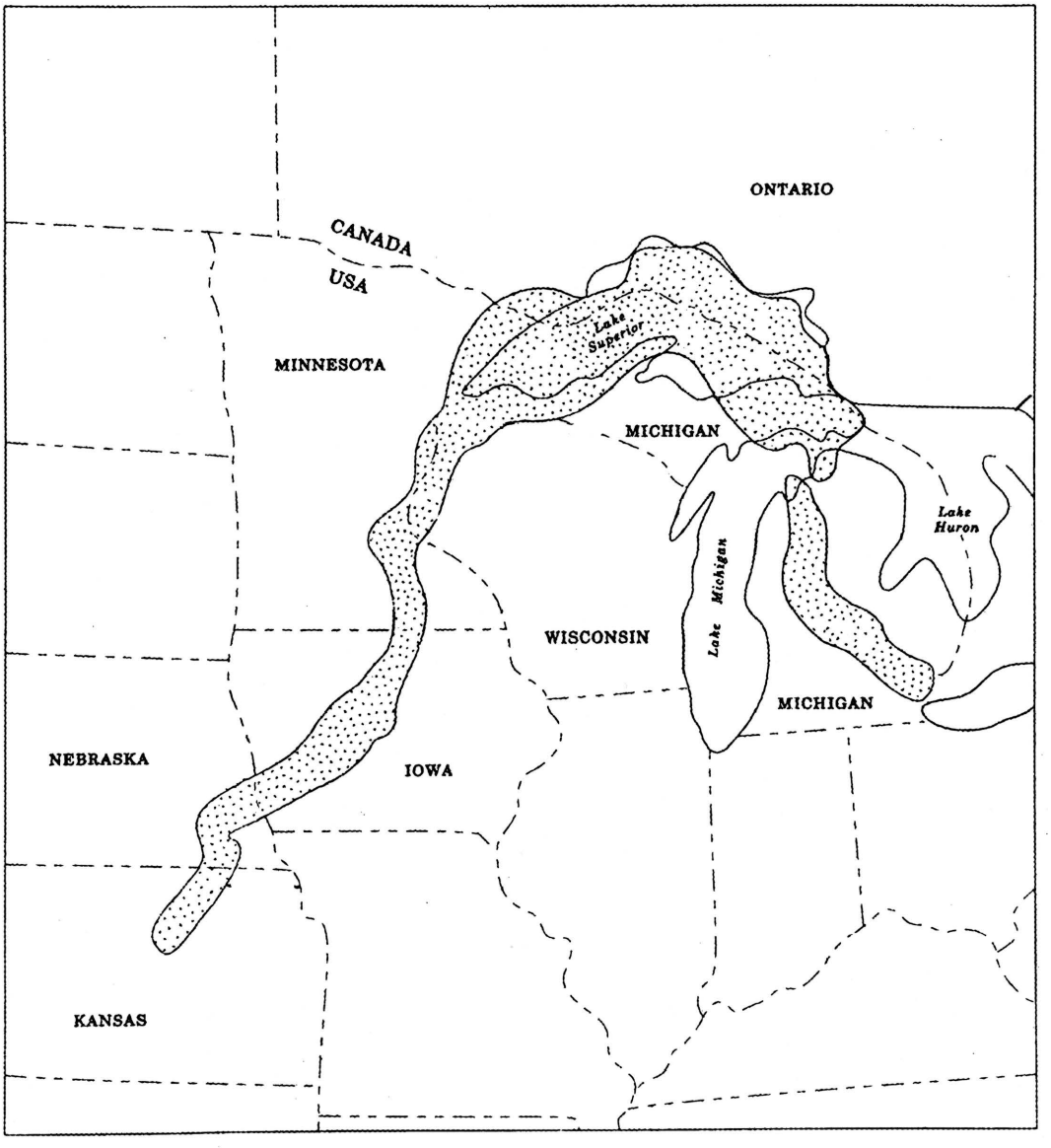

Figure 2.1 Map showing general trend of Mid-continent rift system. (After Cannon et al. 1989)

note the presence of the South East Nebraska Arch (Fig. 2.2), a Precambrian arch that extended as far south as Wabaunsee county, Kansas.

Interpretations of what happened after the formation of the Southeast Nebraska arch vary between downdrop and uplift. After the deposition of the St. Peter Sandstone (Middle Ordovician) but before the Desmoinian, the traditionally held viewpoint (e.g. Lee, 1943; Lee, 1956; Merriam, 1963) suggests the entire region went through a down-warping phase. This downwarping formed the North Kansas Basin (Fig. 2.2). The Nemaha uplift was then uplifted post-Mississippian and pre-Desmoinian. This uplift divided the North Kansas Basin roughly in half creating the present day Salina and Forest City basins (Fig 2.3). Oolites and oxidized shale present within the Chattanooga Shale (Upper Devonian – Lower Mississippian) along parts of the Nemaha uplift, have been used as evidence to suggest that at during at the time of deposition of the Chattanooga Shale, the Nemaha uplift was a positive feature (Berendsen and Blair, 1995). Because the oolites and oxidized shale occur during a time consistent with the occurrence of the downwarping phase, the existence of the North Kansas basin has been questioned (Berendsen and Blair, 1996). This implies that the Nemaha uplift and the South East Nebraska arch may be the same feature that has been a positive feature since Precambrian time (Berendsen, personal communication, 1999).

It is generally accepted that the majority of uplift presently observed on the Nemaha uplift occurred during late Mississippian time and extended into the Pennsylvanian. This movement was coincident with the Ouachita orogeny and seems to be directly related to the orogeny (Berendsen and Blair, 1995). Collision of the two plates in present day southern Oklahoma resulted in a stress field that reactivated existing NE and NW trending faults that formed during rifting. A wrenching motion has been interpreted by some researchers (i.e., Seyrafian, 1978; Berendsen and Blair, 1986) along the Nemaha uplift/Humboldt Fault zone. This wrenching motion has yielded a set of anastomizing faults that have created sets of fault blocks all along the Nemaha uplift with left lateral displacement occurring along NW trending faults (Fig. 2.4). Because the Humboldt Fault zone represents the majority of displacement along the eastern edge of the uplift, the wrenching motion has supplied the driving force for the majority of displacement of the Humboldt Fault zone.

It is important to note that figure 2.4 is the latest interpretation of the regional basement faulting in northeastern Kansas (Bernedsen and Blair, 1996). Originally, the eastern edge of the Nemaha uplift was interpreted to be bound by essentially one long discontinuous fault, named the Humboldt fault. In his map of the Precambrian surface, Cole (1976) interpreted no faults crossing the profile of study. More recent studies have defined the Humboldt Fault as a zone or swarm of faults (e.g. Dubois, 1978; Steeples et al., 1979, Steeples, 1982). However, with the limited

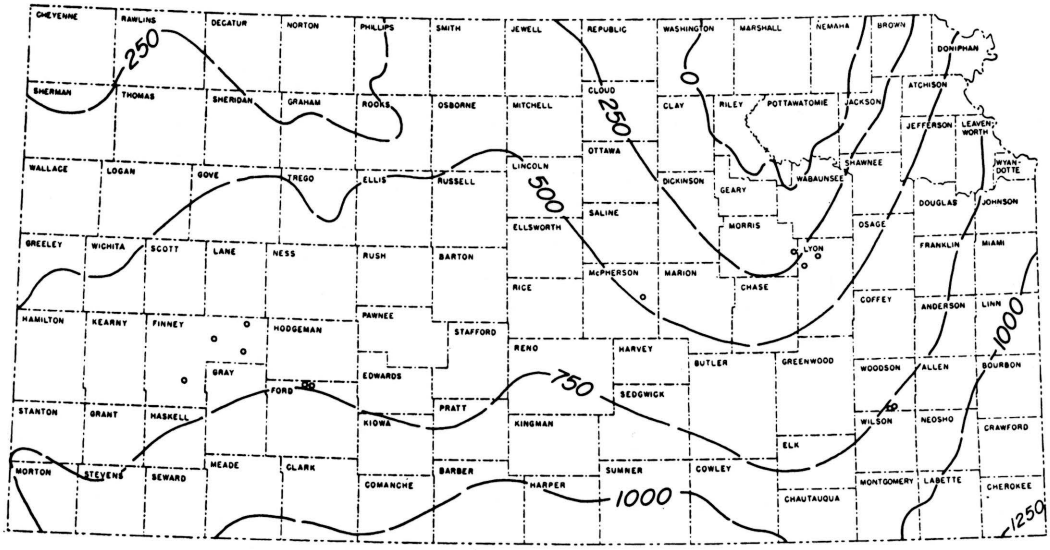

Figure 2.2 Isopach map showing convergence between the tops of Arbuckle rocks tops of Precambrian rocks. The zero contour indicates the extent of the Southeast Nebraska arch. Contour interval is 250 feet. (From Merriam, 1963)

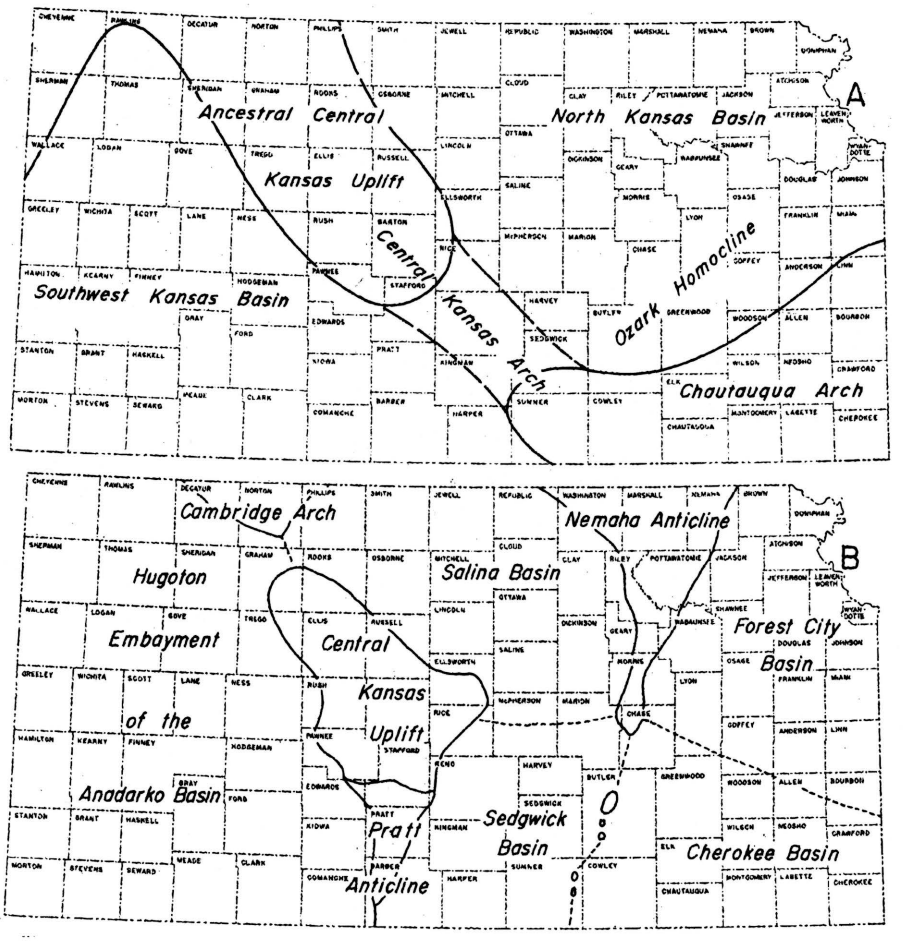

Figure 2.3 Structural development of major Kansas structures: A) pre-Mississippian, post-Devonian; B) pre-Desmoinesian, post-Mississippian. (From Merriam, 1963)

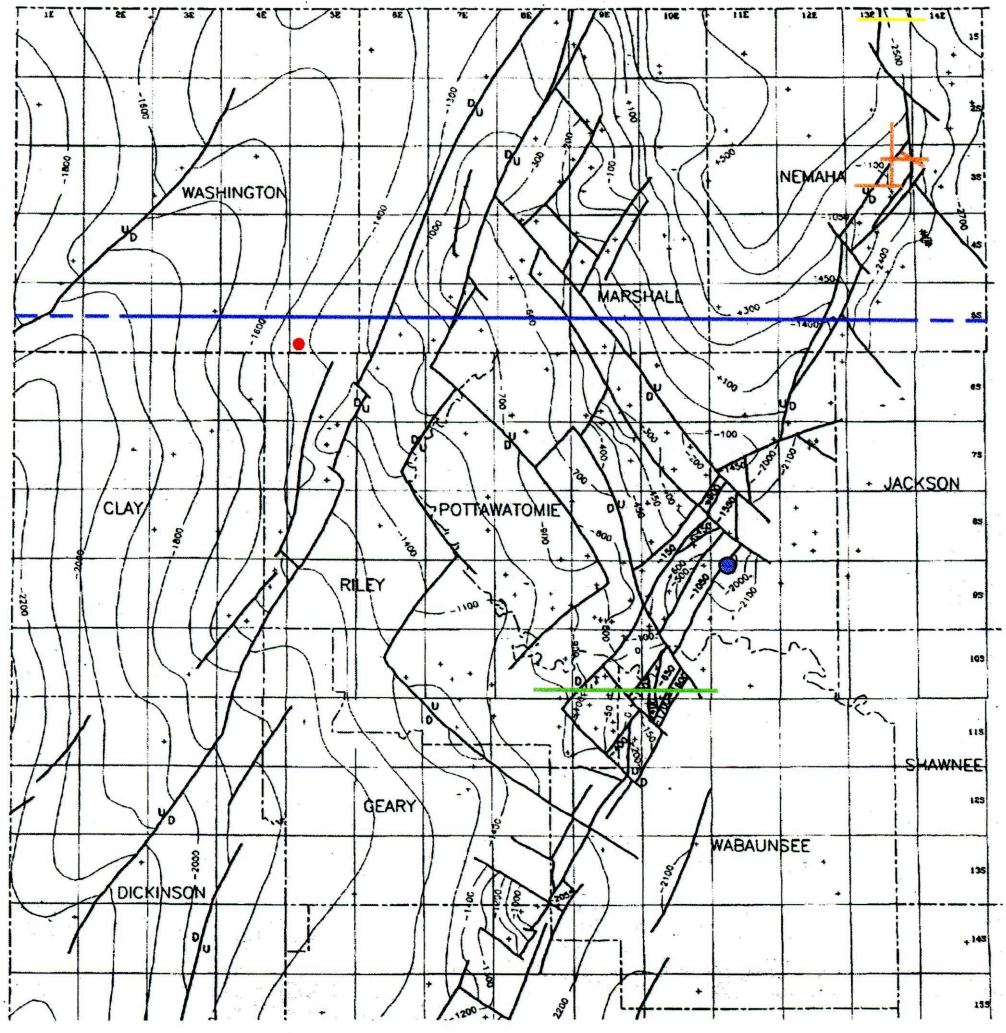

Figure 2.4 Map showing study area and surrounding counties. Dark black lines indicate faults, light black lines indicate contours on top of Precambrian aged rock. All faulting is inferred from well data. Colored line represent; location of the profile of study (bright green); COCORP data (blue); data reviewed by Steeples (1989) (orange); and study conducted by Stander (1989) (yellow). The red dot indicates the approximate location of the Poersch 1 deep drill core. Blue dot shows position of well with repeated section (Seyrafian, 1978). (Base map from Berendsen and Blair, 1996)

number of geophysical surveys in this area, most of the faults associated with the Nemaha uplift, most notably the Humboldt Fault zone, have been interpreted from well data with none of the fault planes having been cut by the wells (Fig. 2.4). Geophysical imaging increases the confidence in structural interpretation inferred from drilling.

2.2 Geophysical Investigations

Regional and localized geophysical studies have provided insight into the structural significance and framework of the Humboldt Fault zone. From a regional perspective, the rifting process has left a major structural imprint on the basement in North-Central Kansas. Many site-specific geophysical investigations of the Humboldt fault zone in North-Central Kansas have provided unique images of local features.

2.2.1 Regional Studies

The most geophysically enlightening of the regional geophysical studies was Consortium for Continental Reflection Profiling (COCORP) which collected over 300 km of deep seismic-reflection data in northeastern Kansas between 1979 and 1981. Data were collected along an east-west profile traversing the Humboldt fault zone and the Mid-continent rift (Fig. 2.4). Original interpretations of this data postulated that the rifting caused primarily down to the east normal faults. As these faults attained greater throw, the faults rotated thus producing low angle normal faults (Fig. 2.5) (Serpa and others, 1989).

In 1984-85 the Texaco 1 Poersch borehole was drilled to a depth of 3440 m in Washington County, KS (Fig. 2.4). This borehole sampled crustal rocks associated with the Mid-continent rift system (Berendsen and others, 1988) encountering a possible reverse fault. Utilizing these data along with gravity and magnetic profiles, the COCORP data were reinterpreted (Woelk and Hinze, 1991). Basin bounding reverse faults were interpreted on either side of the rift (Fig. 2.6). Suggesting an initial period of extension created down to the basin normal faulting which was followed by a compressional stress regime. The compressional stress caused existing normal faults to reverse throw several thousands of feet. This interpretation is not only consistent with the borehole data is consistent with other interpretations of the rift further north (e.g. Cannon and others, 1989). Models fit reasonably well with observations on gravity and magnetic profiles (Fig. 2.6).

2.2.2 Detailed Studies of the Nemaha uplift/Humboldt Fault zone

A 55km long magnetic profile in Pottawatomie county, roughly 35 km to the north of this study, used 100 m station spacing over the length of the profile, but concluded that 500 m station spacing was sufficient to see the "necessary detail" (Konig, 1971). However, only one fault was interpreted with a second possible fault being suggested. Berendsen and Blair (1996), interpret as many as five faults across Konig's profile. This may simply show a shift in geoscientist bias as to

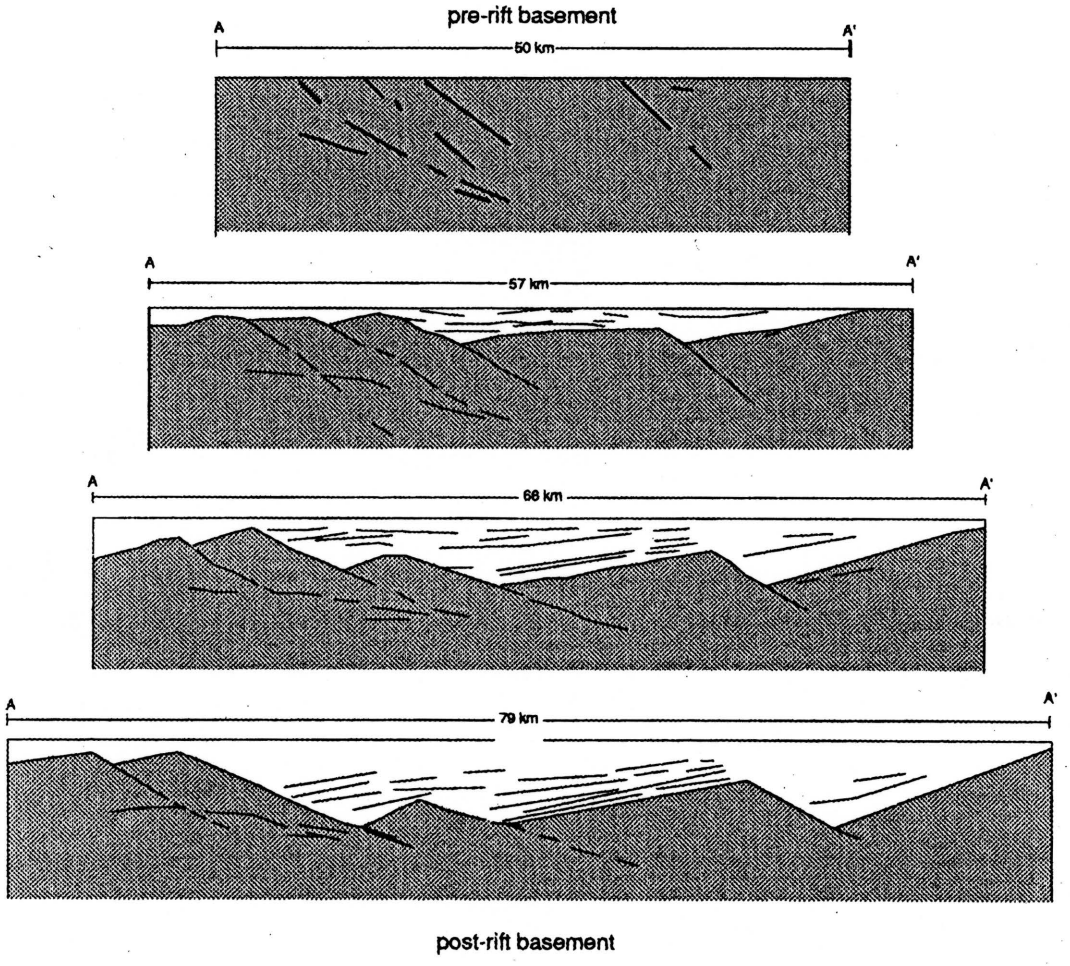

Figure 2.5 Original interpretation of faulting associated with the Mid-continent rift in NE Kansas. (From Serpa et al., 1989)

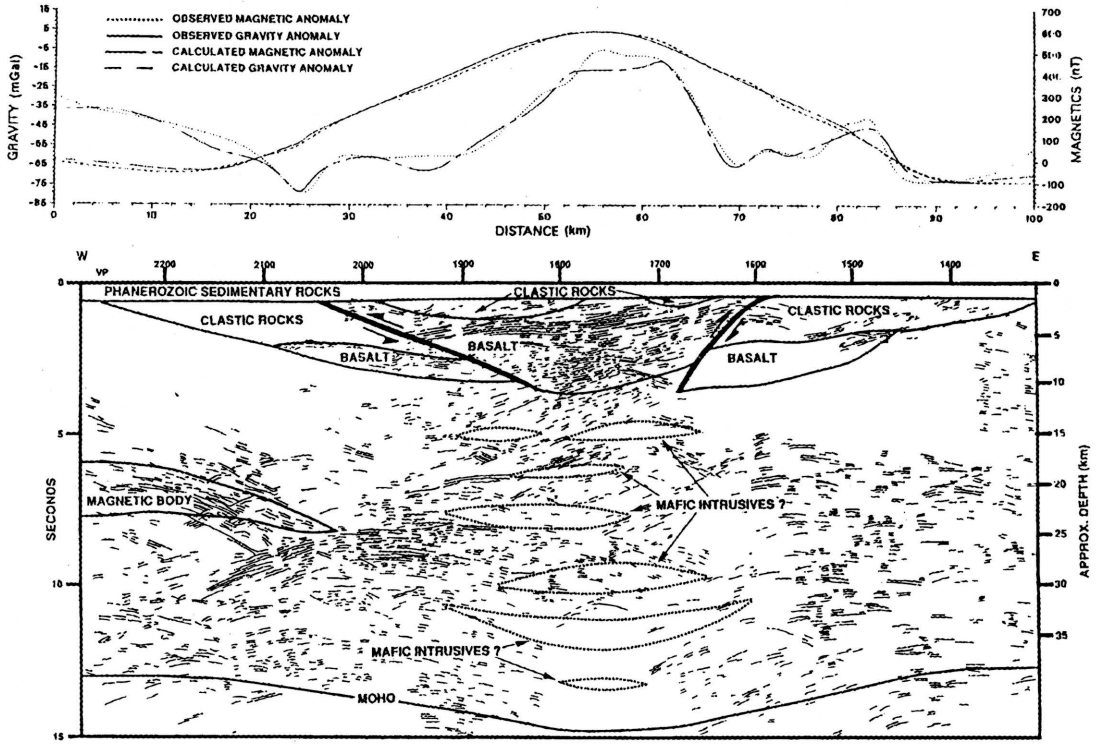

Figure 2.6 Re-interpretation of COCORP data with gravity and magnetic data. Gravity and magnetic model are shown compared with observed data. (From Woelk and Hinze, 1995)

the nature of the Humboldt fault zone or a limitation on the magnetic data because of the small throw (< 80 m maximum in the basement) on three of the faults.

Early researchers interpreted the Humboldt fault as a single fault (Cole, 1976). Though Konig's interpretation may be correct, if the current study suggests multiple faults in the Wabaunsee and Riley county areas, the reinterpretation of Konig's data (Berendsen and Blair, 1996) may be given more credence with even a more detailed re-examination in order.

Another study (Baysinger, 1963) magnetically mapped large portions of Wabaunsee, Riley, and Geary counties. This study, however, is of limited use for detailed interpretation of smaller structures because of the large station spacing (1/2 mile) along the traverses and the traverses occur rather sporadically over the study area with sections as large as 8 square miles which do not include stations.

A few very localized seismic studies have been conducted over the Humboldt Fault zone (e.g. Steeples, 1982; Steeples, 1989; Stander, 1981; Stander, 1989). Seismic sections from Nemaha county (Fig 2.4) collected and processed by Cities Service show a series of faults dipping northwest and southeast with one possible reverse fault (Steeples, 1982). This interpretation strongly suggests that the Humboldt fault zone is a complex set of faults with changing stress regimes. Seismic data from northern Nemaha county (Fig. 2.4) suggests a single large east dipping normal fault (Stander, 1981). These different but compatible interpretations may suggest significant lateral variations in the fault character. However, the northern Nemaha county seismic data does not penetrate the pre-Pennsylvanian sedimentary section. Therefore, interpretations of this data cannot comment on the pre-Pennsylvanian stress field.

3. Potential Field Data Acquisition and Processing

A gravity and magnetic profile were collected along the seismic profile using a Lacoste and Romberg model D gravity meter and a Geometrix G856 Proton precession magnetometer (Fig. 3.1). Stations spacing is at 0.32 km (0.2 mi) on the ends of the profile and 0.16 km (0.1 mi) in the center (Fig. 3.1). One base station was used for the entire survey (Fig. 3.1) with visitations once every hour and a half. No attempt was made to tie these data into known gravity and magnetic stations, thus this survey was purely relative. A U.S.G.S. 7.5 min. topographic map provided north-south directional control and elevation information. The majority of the profile is flat with maximum slopes on the order of 40 m/km occurring at the east end of the survey, but with average slopes around 1m/km along the western ¾ of the profile (Fig. 3.2) making topographic map-read elevations accurate within 1.5 meters (5 ft) using this method. A vehicle odometer was used for for east-west location control. Data were collected along Kansas highway 18.

With only 140 stations in each data set, Microsoft Excel was easily capable of processing these data. Corrections applied to the gravity data (Fig. 3.3) were:

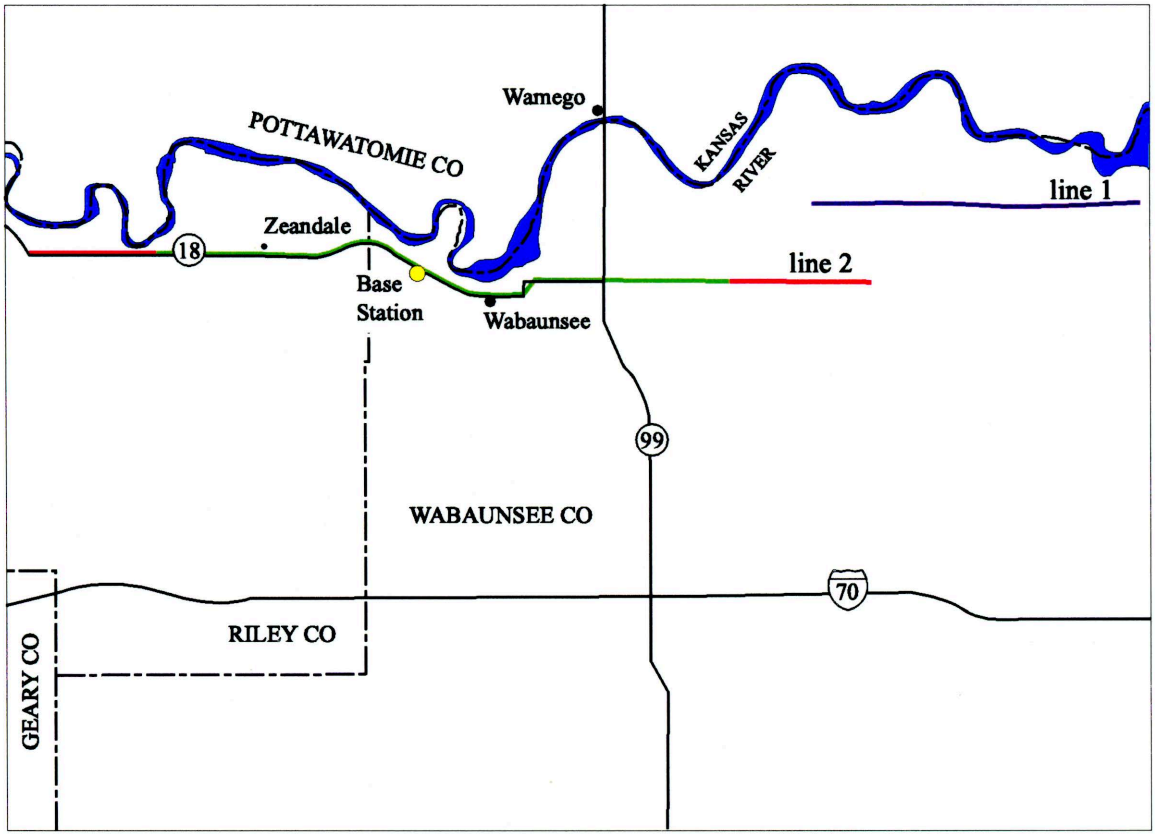

Figure 3.1 Base map of data collected for this study. Line 1, the purple line, represents one of the seismic profiles, and line 2, red and green lines, represents the other seismic profile, as well as the magnetic and gravity profiles. The red portions of line 2 show where potential field data was acquired at 0.2 mile (0.32 km) station spacing, and the green portion of line 2 represents 0.1 mile (0.16 km) station spacing for the potential field data. The yellow dot shows the location of the sole base station used in the magnetic and gravity surveys.

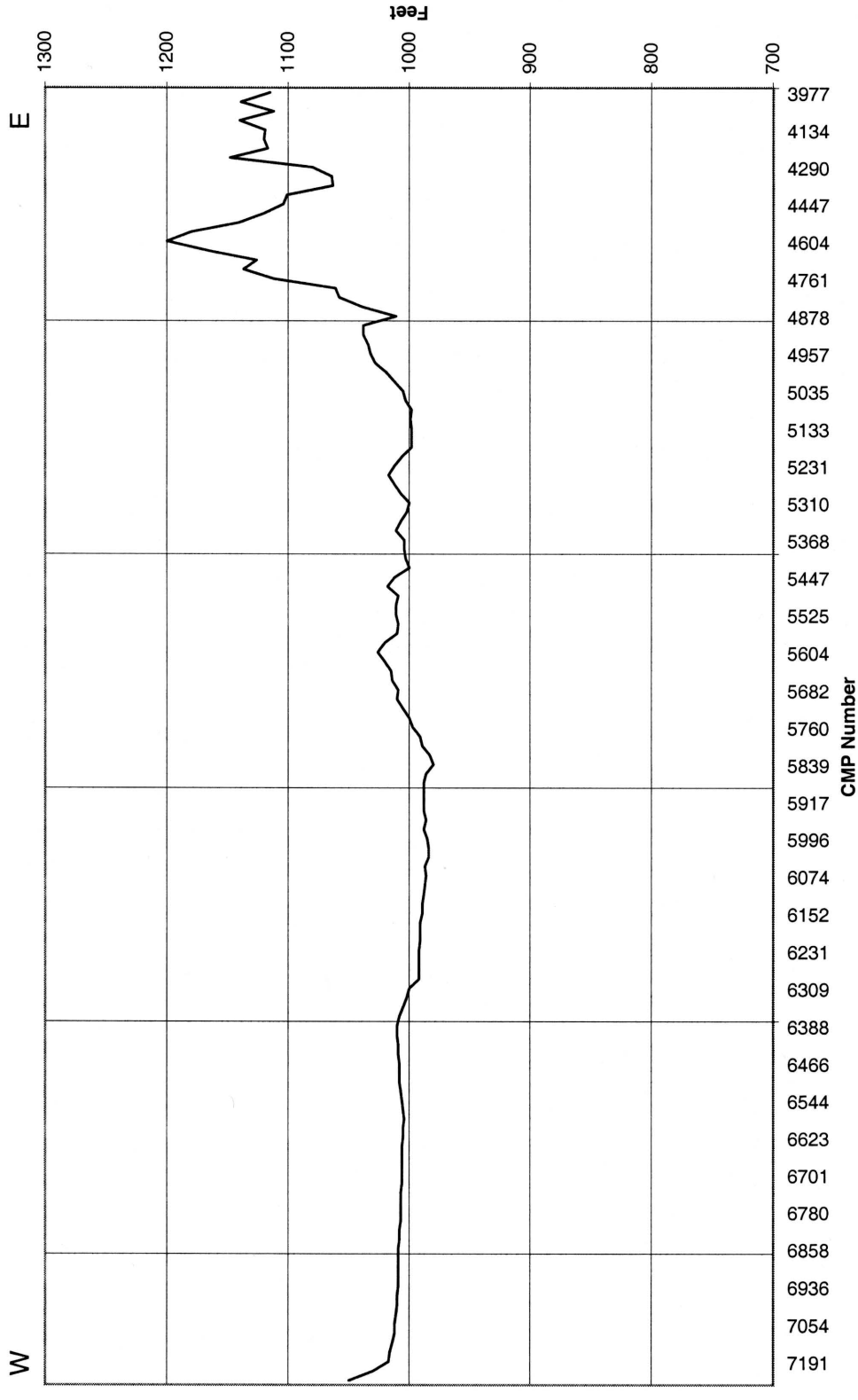

Figure 3.2 Elevation along the gravity and magnetic profile. Vertical exaggeration is about 100.

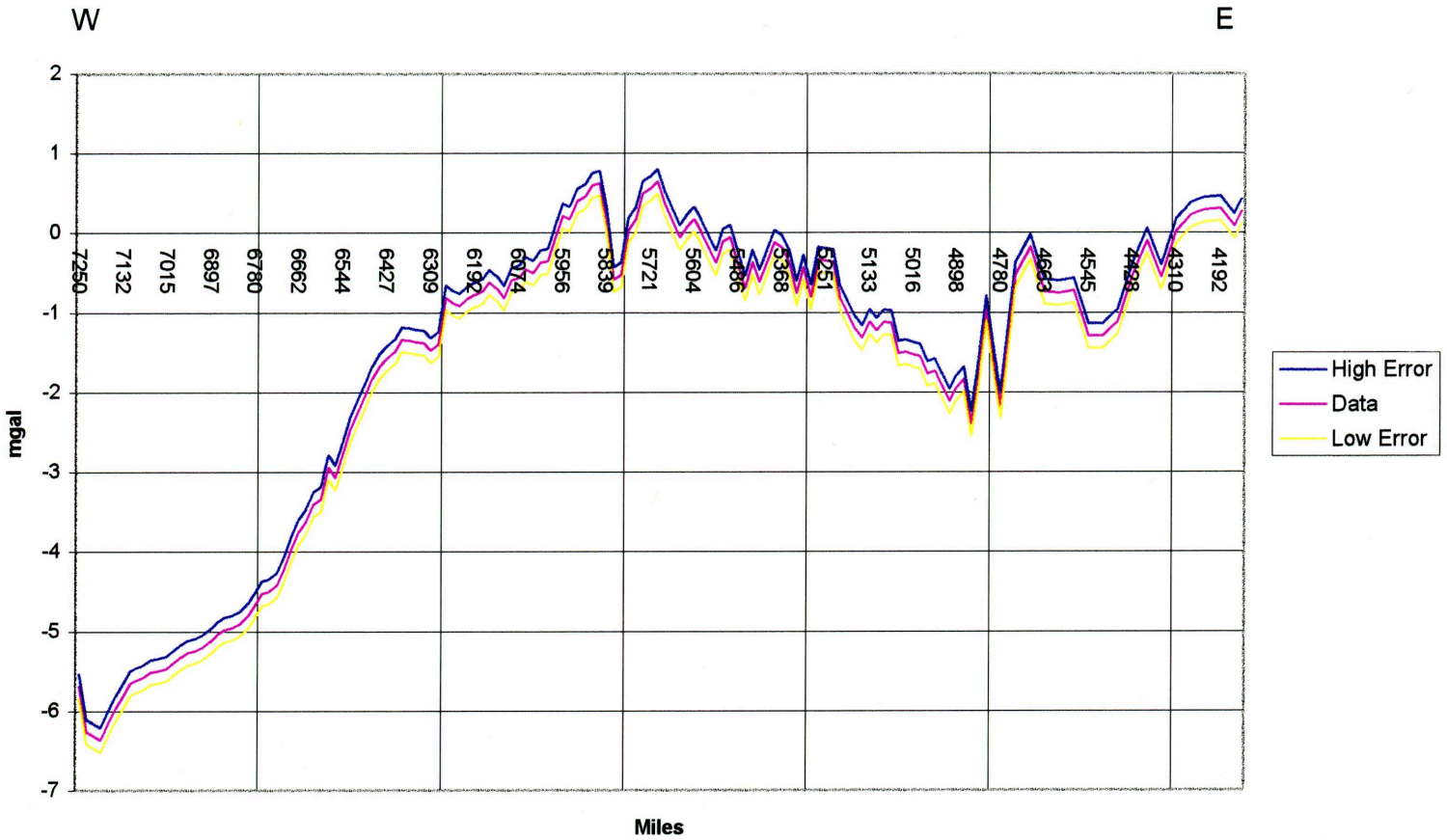

Figure 3.3 Bouguer gravity profile with error envelope across the Humboldt fualt zone / Nemaha uplift system in Wabaunsee and Riley counties, Kansas. Data and error calculations are discussed in the text.

1) Drift correction
2) Latitude correction
3) Free-Air correction
4) Bouguer correction

The magnetic data were only corrected for drift. These corrections and error associated with each correction are consistent with currently accepted practice (i.e. Burger, 1992; Sharma 1986) (Appendix A).

Error estimation for the magnetic data (Fig. 3.4) was limited since only drift was corrected. The error associated with the magnetic drift was calculated in the same manner as the drift error associated with the gravity data. As a check of the validity of using linear interpolation to correct for drift in the magnetic data, GIN data were retrieved from the Golden, Colorado site via the internet. GIN data are magnetic readings taken once per minute at a stationary magnetometer in Boulder, Colorado. Many localities are available though the Golden GIN, however, the Boulder site was selected due to its close geographical proximity to the study area. Linear interpolation between base station readings is a very good approximation for drift corrections (Fig. 3.5).

Additional processing designed to aid in the interpretation of the data. Because data were collected at two different station spacings (0.2 mile spacing at the ends of the line, and at 0.1 miles spacing along the center of the line) data at the ends of the line were linearly interpolated down to 0.16 km (0.1 mi) spacing. Following the linear interpolation, first derivatives of both data sets were calculated using a middle derivative method:

$$D_{y_n} = \frac{y_{n+1} - y_{n-1}}{2x}$$

$$x = station\ spacing$$

$$y_n = data\ value\ at\ station\ n$$

Using first derivative data, instantaneous slopes of the data become better defined and even subtle changes in slope are easier to recognize (Figs. 3.6 & 3.7).

A 3-term running average was calculated for both data sets to minimize significant amounts of small wavelength noise existing in the data, especially the magnetic data. The running average has the effect of filtering high wavenumbers from the data and thus has a smoothing effect. Lower wavenumbers that remain are more indicative of the gross regional structures. After the running averages were calculated, middle derivatives were again calculated for the data (Figs. 3.8 – 3.11).

The first order trend was removed to extract regional effects on the data (Fig. 3.12 & 3.13). A linear trend fit to the gravity data suggests slopes that are upward to the east (Fig. 3.3). This observation is expected from for the Moho in this part of the state (Xia and Sprowl, 1995). The

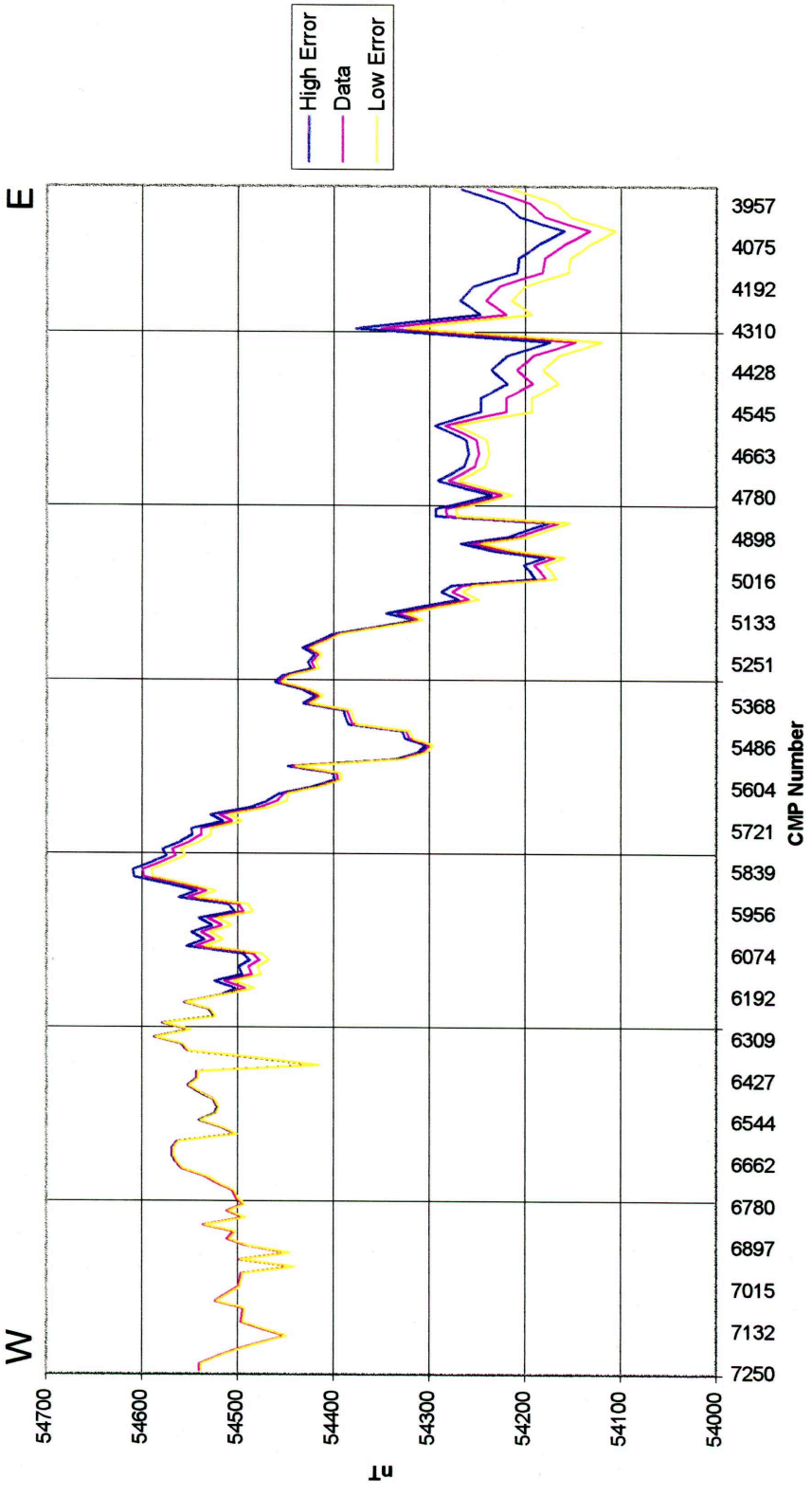

Figure 3.4 Magnetic data with error envelope of profile across Humboldt fault zone / Nemaha uplift in Wabaunsee and Riley counties, Kansas. Data and error calculat discsussed in the text.

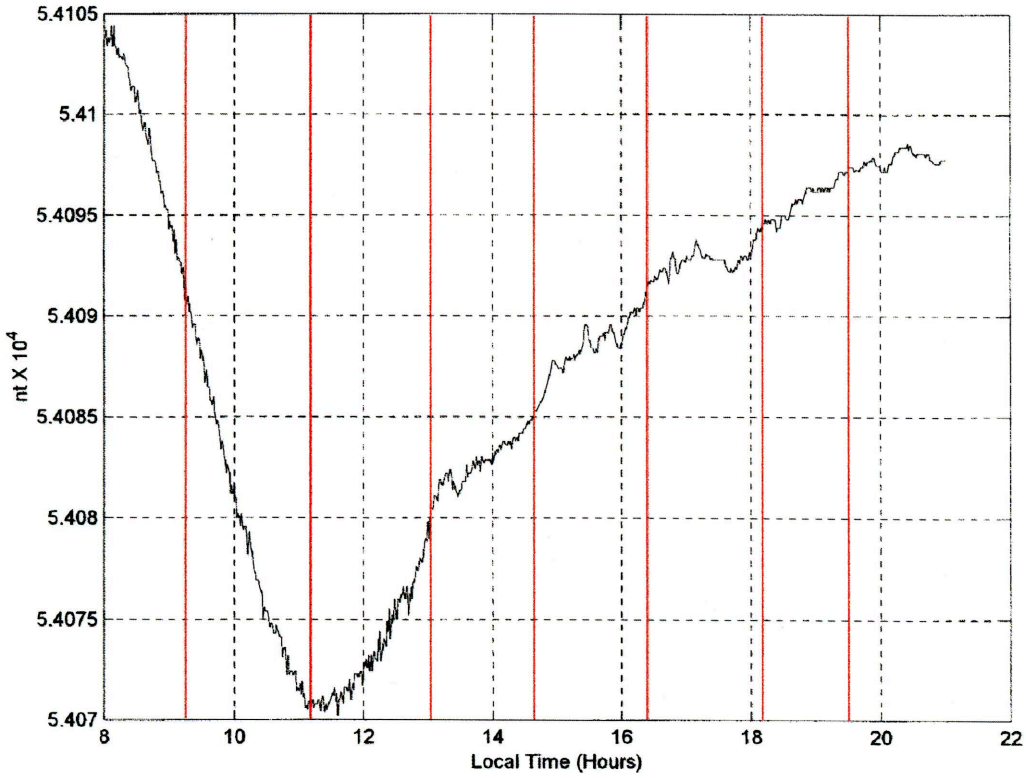

Figure 3.5 Magnetic field changes at Boulder, Colorado on April 12, 1999. The magnetometer used to collect this data was at a stationary location, and data were recorded once per minute. Red lines indicate times when base station readings were acquired. As can be seen, linear interpolation among base station readings will yield a good approximation for the drift correction.

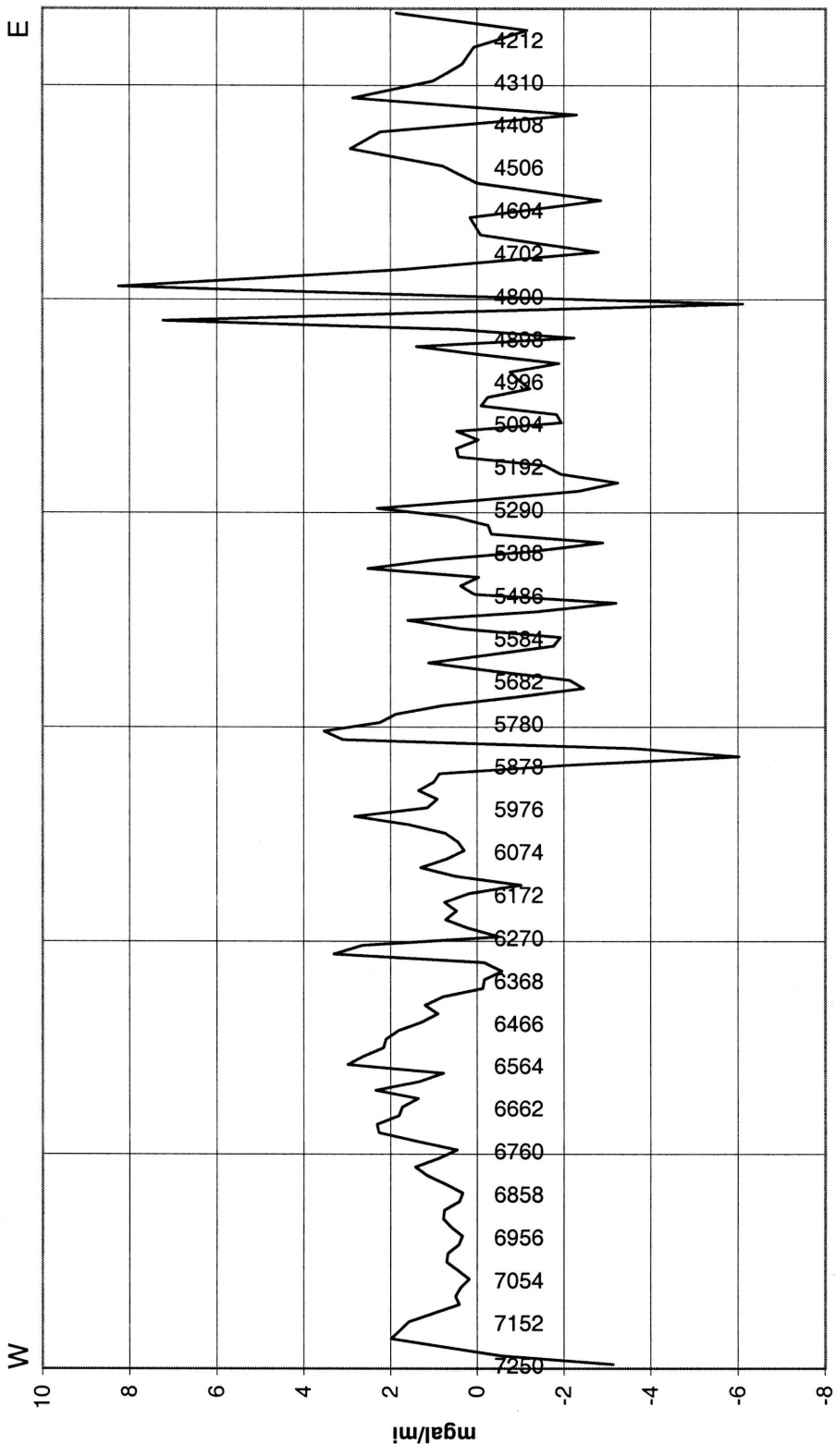

Figure 3.6 First derivative of Bouguer gravity data. Data correspond to figure 3.3.

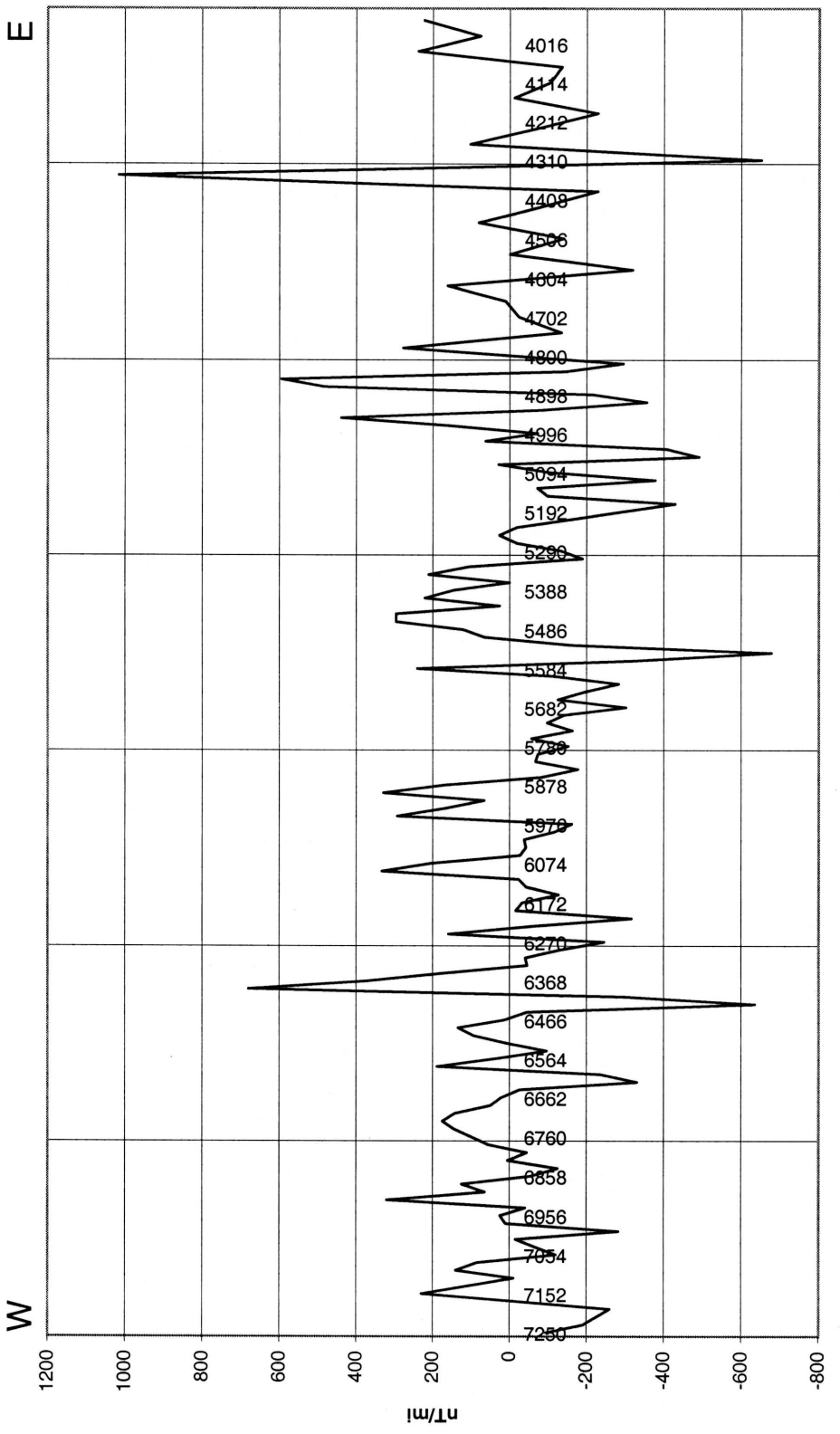

Figure 3.7 First derivative of magnetic data. Data correspond to figure 3.5.

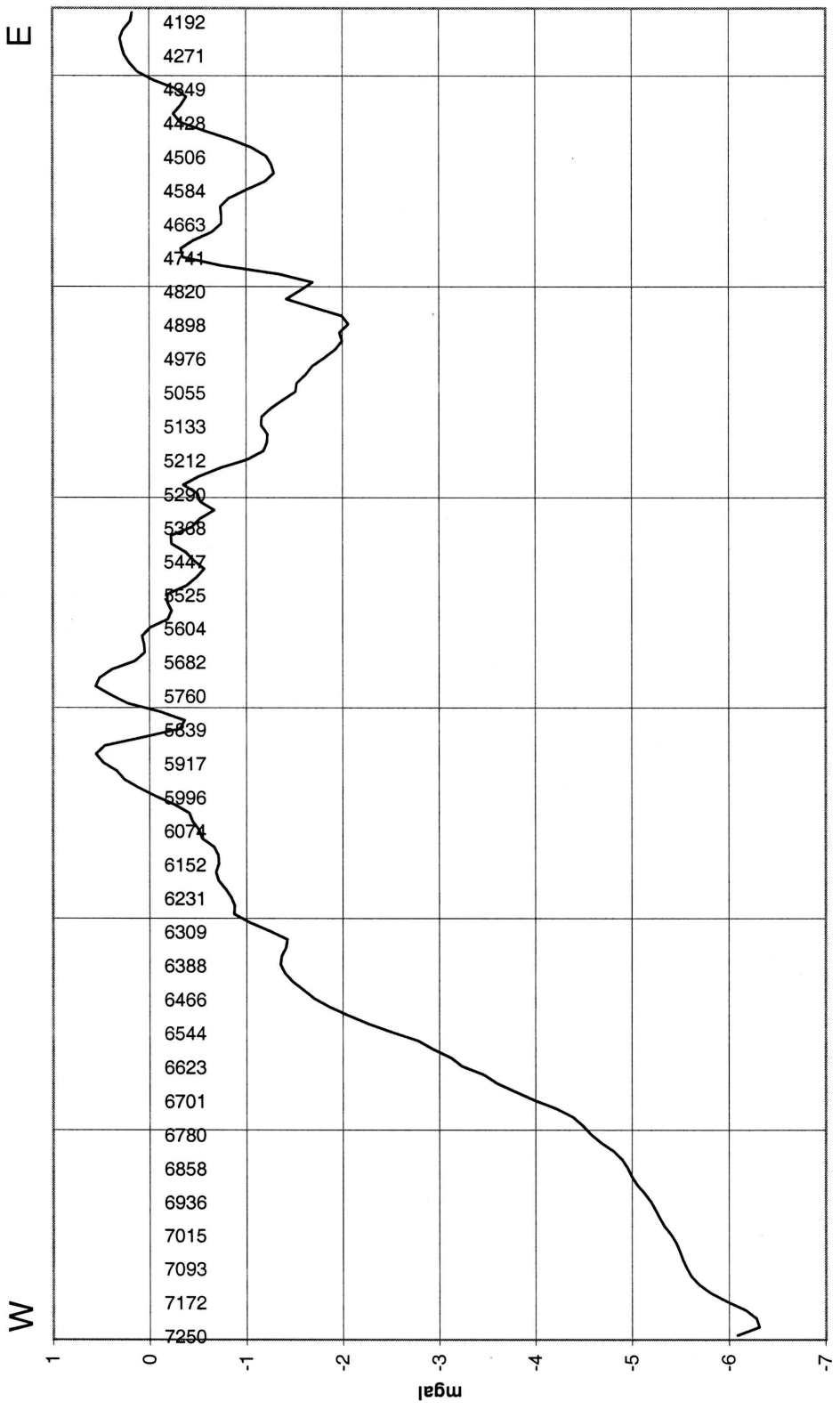

Figure 3.8 Three term running average of Bouguer gravity data. Data correspond to figure 3.3.

Figure 3.9 Three term running average of magnetic data. Data correspond to figure 3.5.

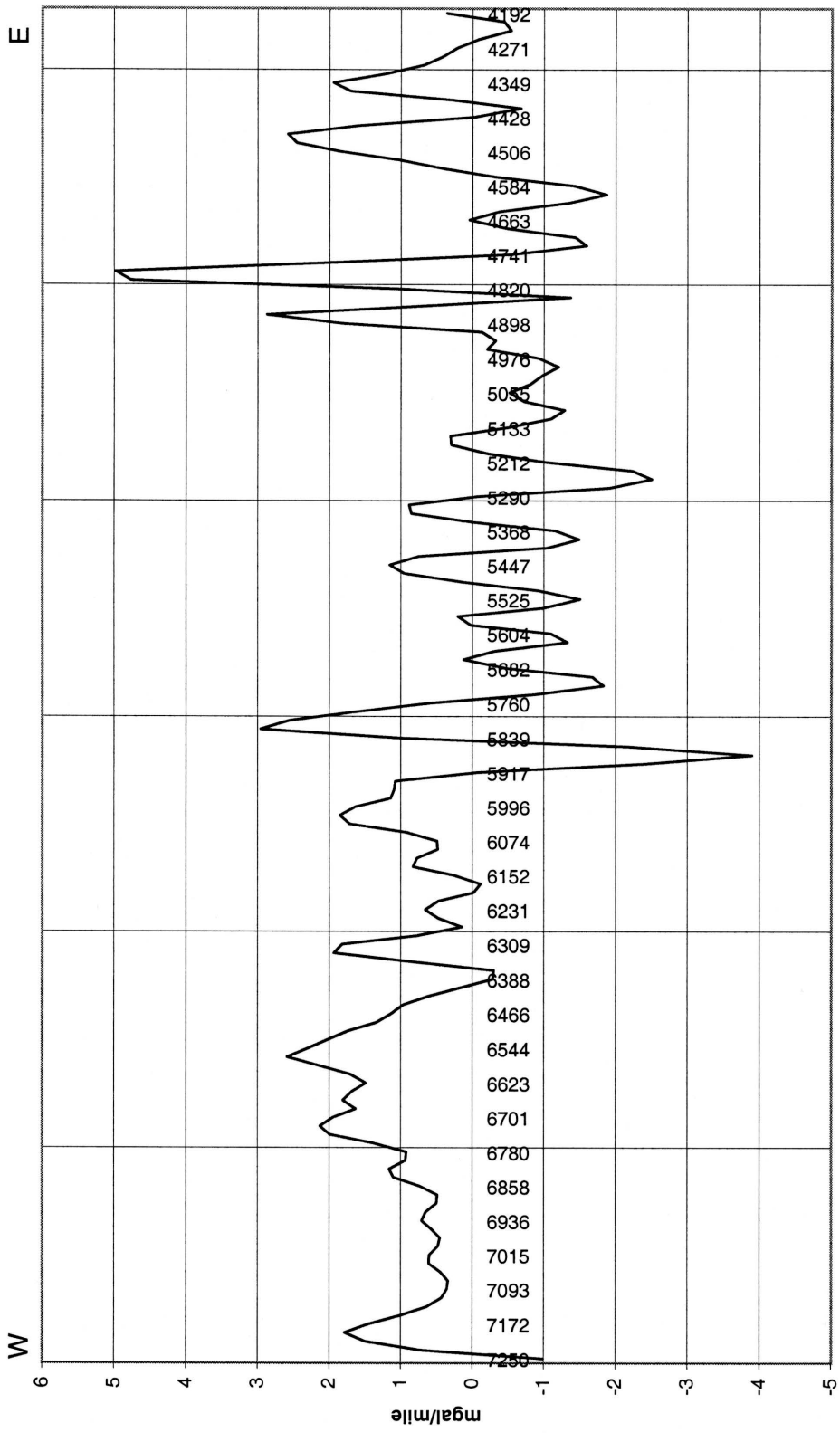

Figure 3.10 First derivative of Bouguer gravity data three term running average. Data correspond to figure 3.8.

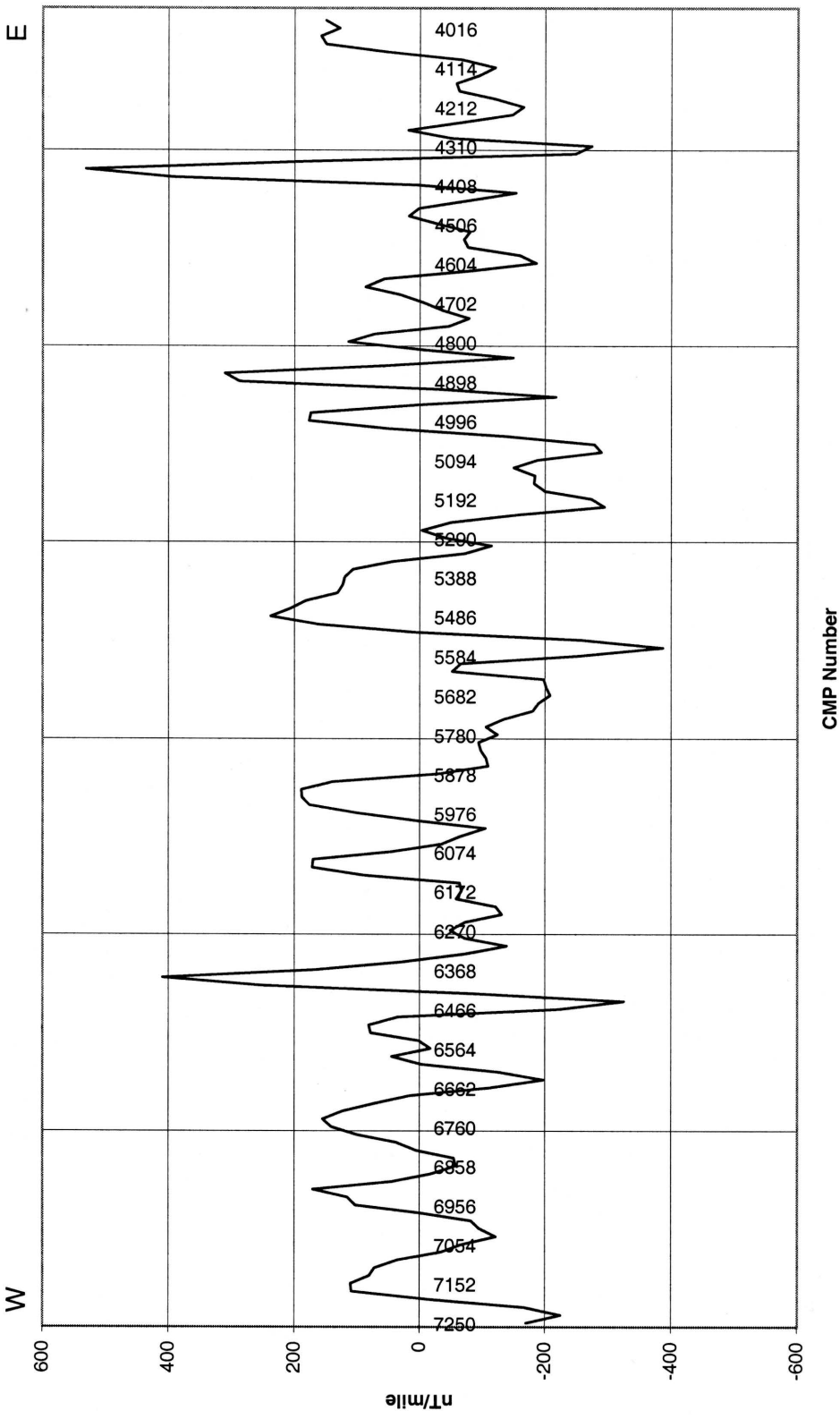

Figure 3.11 First derivative of magnetic data three term running average. Data correspond to figure 3.9.

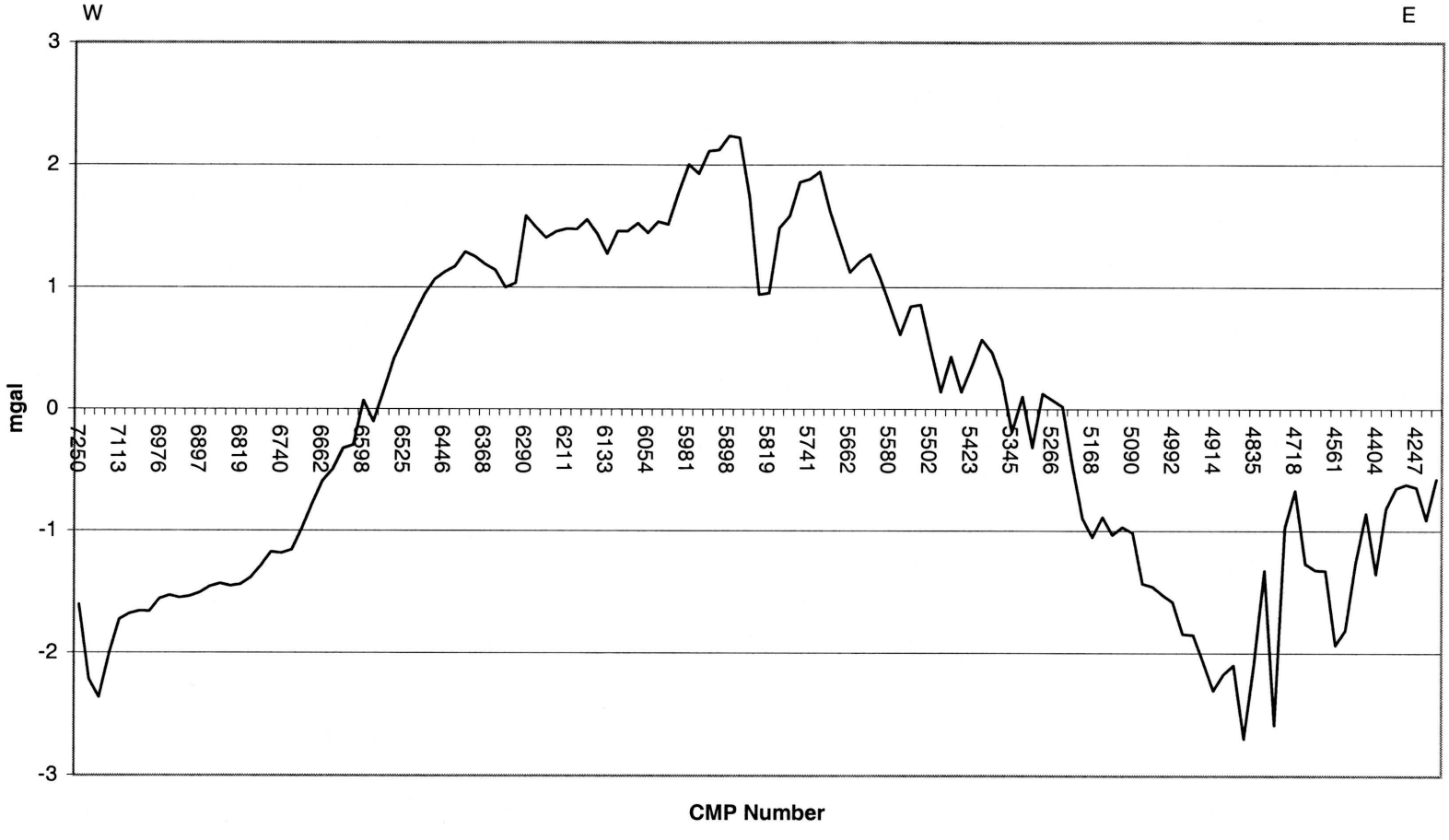

Figure 3.12 Gravity data wih first order trend removed. The Nemaha uplift becomes much more apparent in the data because the first order trend is characteristic of changes in the depth to the Moho.

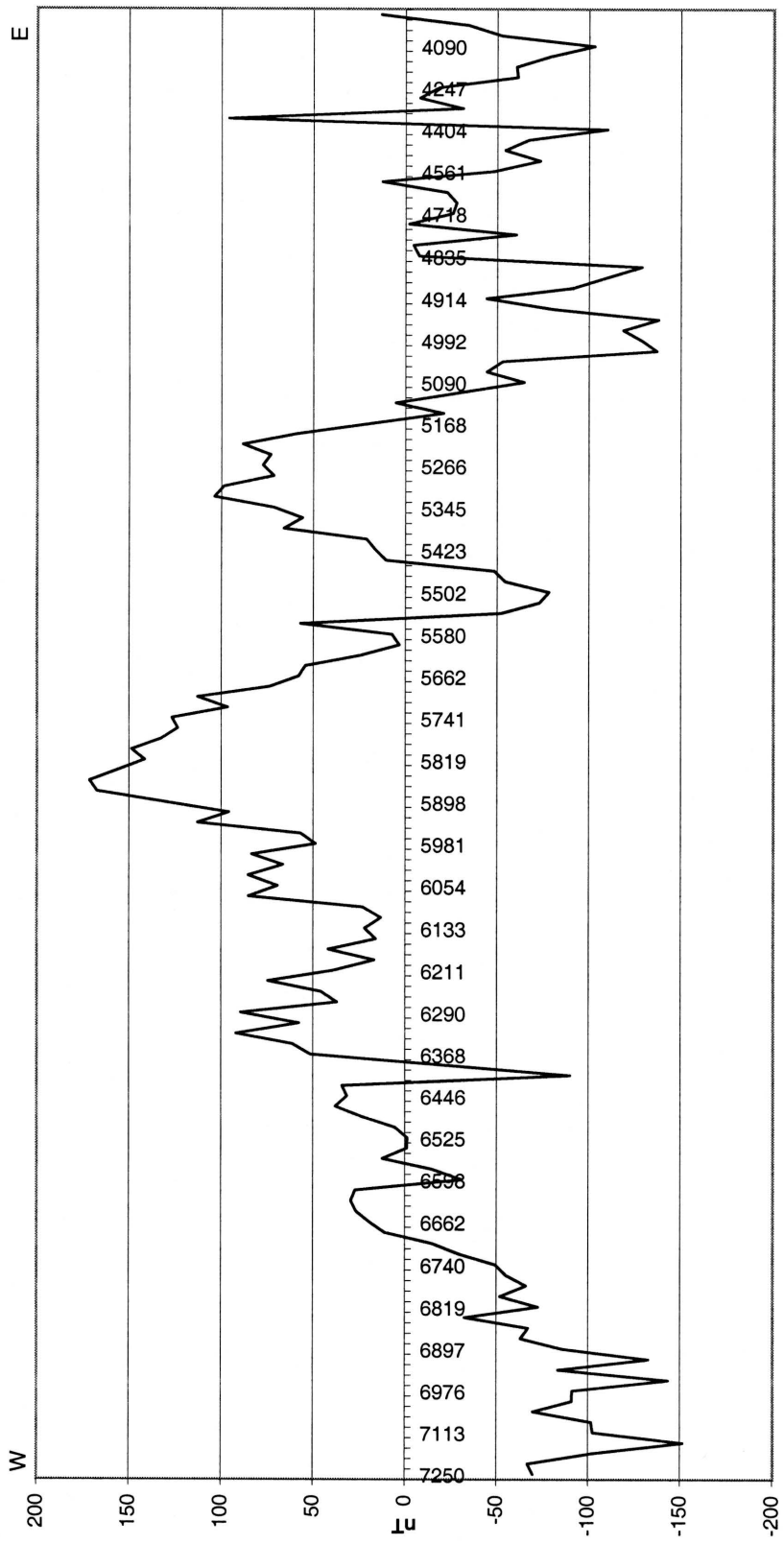

Figure 3.13 Magnetic data with first order trend removed. The Nemaha uplift, as well as the Humboldt Faul zone, become more apparent.

linear trend of the magnetic data slopes in the opposite direction. Removing this trend enhances shallow events helping to illuminate the Nemaha uplift (Fig. 3.12 & 3.13).

4. Seismic Data

Two east-west near-surface 2-D seismic profiles were collected in Wabaunsee and Riley counties (Fig. 3.1) in July and August 1997 to image the Humboldt fault zone. The profiles were collected with an east/west overlap of about 1.6 kilometers and separated by roughly 2.4 kilometers. The asymmetric split-spread profiles were designed to represent a single dip-line traverse across the Humdoldt Fault zone. The offset was necessary due to a limited number of east-west roads traversing the entire proposed profile area. Cumulative length of the two profiles is 35 km with the longer western profile passing through the towns of Wabaunsee and Zeandale, Kansas, hence this seismic data set has been referred to as the Zeandale line. The shorter eastern profile is referred to as line 1, the western profile as line 2. Because line 1 is entirely in the Forest City Basin, it is not interpreted or dealt with in the text. It does, however, appear un-interpreted as Plate A.

An IVI Minivib-1 seismic vibrator was used as a source (Geyer, 1969). The vibrator sweep was a 20-200 Hz 10 second upsweep. Three upsweeps were run at each source point. Source spacing along the length of the profile was 55 feet. Geophone arrays were one meter across and consisted of three forty Hertz vertical geophones wired in series spaced on 55-foot centers. Because source points were located between geophone stations the nearest source offset was 27.5 feet. The nominal fold for the data across the profile was forty, but the fold varies from twenty to sixty along the west half of line 2.

Winseis® processing software developed at the Kansas Geological Survey for use on PC's was used to process (Table 4.1) the Zeandale seismic data.

Powerline noise was prevalent along many parts of the line. A Hum filter was used to attenuate much of the 60 Hz power-line noise (Xia and Miller, 1997). This filter is designed to remove sinusoidal noise from the data. Data quality was improved 100% of the time the Hum filter was applied regardless of where the Hum filter was applied in the processing flow. However, testing of the application the Hum filter pre-correlation and post-correlation on different vibroseis data sets indicated 75% of the time the pre-correlation application of the filter would produce better results than the post-correlation application. The Hum filter uses a pre-first arrival quiet zone to estimate the amplitude and phase of sinusoidal noise. Sources of noise other than cyclical powerline noise are present pre-first arrival in most of the instances that the Hum filter was ineffective. These other noise sources (i.e. trucks driving by, somebody walking on the line, an airplane flying over, etc...) likely cause a misestimation of the sinusoids amplitude and phase. The Hum filter was run on the uncorrelated data at 60, 120, and 180 Hz. However, a test section

Hum Filter (Power Line Noise Eliminator)
Cross-Correlation
Trace Editing
Vertical Stacking
Setup of Field Geometry
Band Pass Filter
Scaling
Elevation Statics
Muting
Sorting into Common Mid-Points
Velocity Analysis
Normal Moveout Correction
Surface Consistent Residual Statics
Residual Statics
Datum Statics
Trace Stacking
Migration Filter (Random Noise Attenuator)
Automatic Gain Control (AGC) Scaling

Table 4.1 Processing sequence for the Zeandale seismic profile.

was processed using exactly the same processing steps and parameters except the Hum filter was applied after correlation as opposed to before. No difference was evident in the final stacked sections. Since uncorrelated data contains considerably more samples than correlated data, application the Hum filter is most efficient with post-correlated data.

Also analyzed was the correlation method and optimum pilot. Traditionally, vibroseis data has been cross correlated with a synthetic sweep. This usually works reasonably well, however there are problems associated with this approach. Vibrators do not behave exactly as they are programmed to. The resultant sweep that is imparted to the ground has phase and amplitude differences with the synthetic sweep (Lerwill, 1981). Harmonic distortions also occur (Seriff and Kim, 1970). Because the sweep used in this survey went from low frequencies to high frequencies (upsweep), any harmonic distortion will be a forerunner. This means that noise due to harmonic distortion will occur in negative time and thus should not degrade the final section (Seriff and Kim, 1970). However, this harmonic distortion can still be considered signal; it is present in the energy that goes into the ground at the vibrator pad contact point. If we can correlation with a sweep which includes the proper harmonic distortion component and the true phase and amplitude component of the sweep, data quality should be improved from correlation with a synthetic or theoretically close (Allen et. al., 1998).

The IVI Minivib is equipped with a single accelerometer on the mass and one on the baseplate. Each time the vibrator sweeps, a file is stored with each accelerometer represented as a trace and the ground force trace. The ground force trace is a weighted average of the baseplate accelerometer and mass accelerometer. In an effort optimize the final correlated shot gathers, tests were run comparing correlation the mass accelerometer trace, the baseplate accelerometer trace, the ground force trace, and a synthetic trace with the data.

Mathematically, the correlation routine may take two forms. Traditional cross-correlation multiplies the amplitude spectra of the out put data and the pilot trace, and the phase spectra are subtracted. The pilot trace may be inverted from the data, though. This procedure consists of dividing the amplitude spectra and subtracting the phase spectra (Smith and Jenkersen, 1998). The resultant data is minimum phase as opposed to cross-correlation that yields mixed-phase data (Yilmaz, 1987). The complete correlation test yielded eight methods of correlation:

1. Cross-correlation with the baseplate accelerometer
2. Inversion of the baseplate accelerometer
3. Cross-correlation with the ground force
4. Inversion of the ground force
5. Cross-correlation with the mass accelerometer
6. Inversion of the mass accelerometer

7. Cross-correlation with a synthetic

8. Inversion of a synthetic

After correlation, each data set was then processed using identical parameters into CMP section (Fig. 4.1a-4.1h). Inversion with the mass accelerometer trace or cross correlation with the mass accelerometer yielded the most coherent reflectors coupled with a high frequency content (Fig. 4.1c, 4.1d). The lowest frequency content was given by the inversion with baseplate accelerometer (Fig. 4.1b), and the least coherent reflectors were produced by cross-correlation with the baseplate accelerometer (Fig. 4.1a). Since the ground force is made up of a combination of the mass and baseplate accelerometer data, it appears that the baseplate portion of the data corrupts or at least degrades the quality of data more than with the mass accelerometer or the synthetic. Unfortunately, only about half of the mass accelerometer files were available for processing. It was therefore necessary to use the next best processing option. Cross-correlation with the synthetic was used to process the entire line.

Elevations of geophone stations and source stations need to be known to determine elevation statics. When the original elevation data was compared with USGS 7.5 minute topographic maps, it was noted that this cumulative error proved to be significant over the course of several miles. Along line 2, this was well over 200 feet. In order to compensate for this error, tie points were chosen along the line and the elevation readings were normalized using elevations read from the topographic maps. This helped to alleviate any error accumulating to any great quantity over the length of the profile.

Migration was not applied to the data three reasons. First, fault diffractions did not appear to be a problem, and in places aided in interpretation of faulting events. Second, migration acts as a low pass filter, narrowing the bandwidth of the data and thus reduces resolution (Ivanov et al., 1998). Third, the maximum dip of reflecting events was about 13 degrees. The relationship between a reflector pre- and post-migration is given by the following equation (Chun and Jacewitz, 1981):

$$\sin(\alpha) = \tan(\beta)$$

$$\alpha = \textit{reflector dip pre} - \textit{migration}$$

$$\beta = \textit{reflector dip post} - \textit{migration}$$

With maximum dips in the range of thirteen degrees, migration will shift events only a fraction of a degree.

Although migration was not applied, migration filtering was used. Migration filtering attenuates high frequency random noise by grossly undermigrating seismic data causing reflection

Following two pages: Figure 4.2 A-H. Brute stackes of vibroseis data that has been correlated eigth different ways: a) Cross-correlation with baseplate accelerometer; b) Inversion with baseplate accelerometer; c) Cross-correlation with mass accelerometer; d) Inversion with mass accelerometer; e) Cross-correlation with Ground Force; f) Inversion with Ground Force; g) Cross-correlation with synthetic sweep; h) Inversion with synthetic sweep.

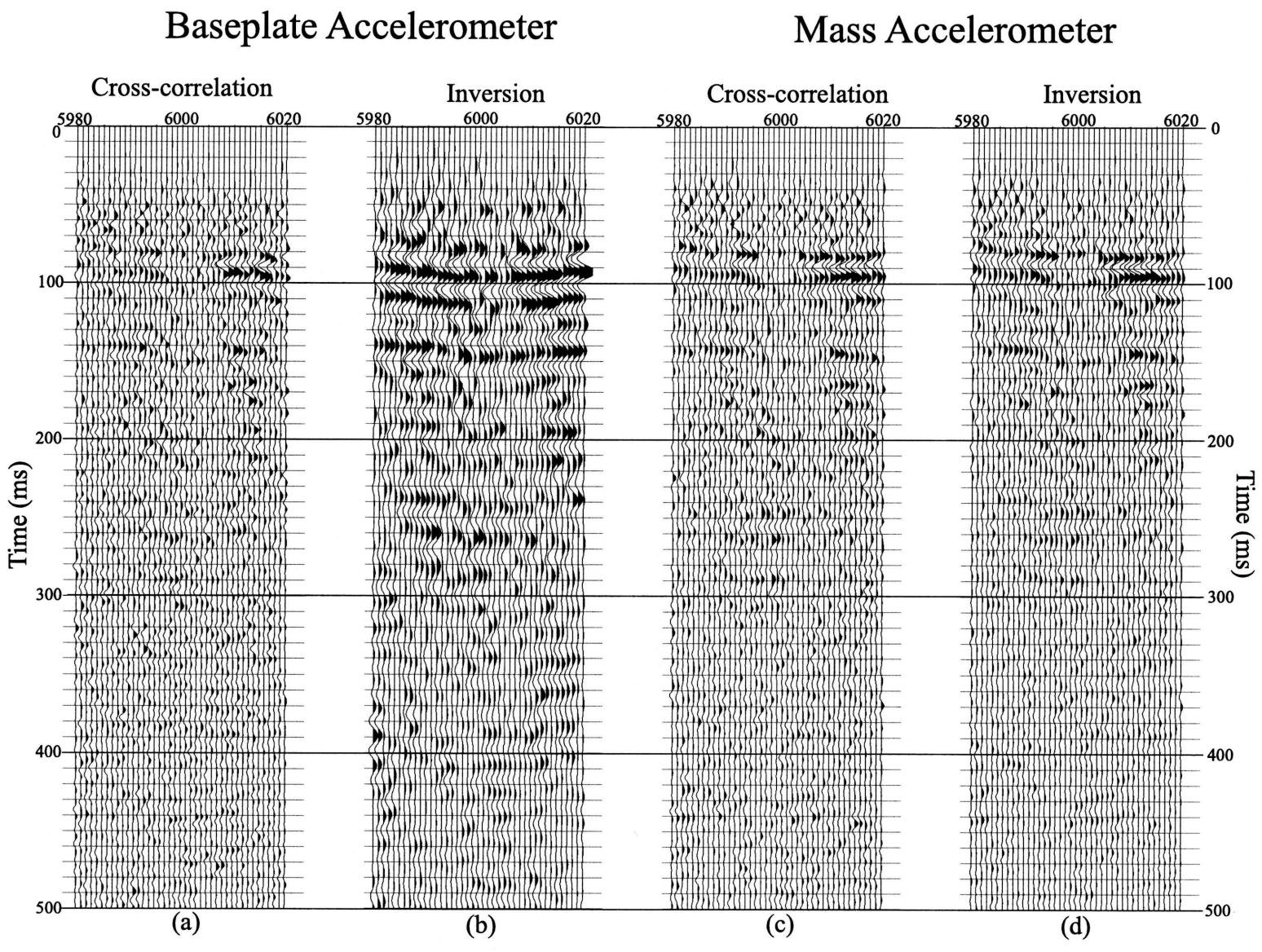
Baseplate Accelerometer
Mass Accelerometer
Cross-correlation
Inversion
Cross-correlation
Inversion
5980
6000
6020
0
100
200
300
400
500
Time (ms)
(a)
(b)
(c)
(d)

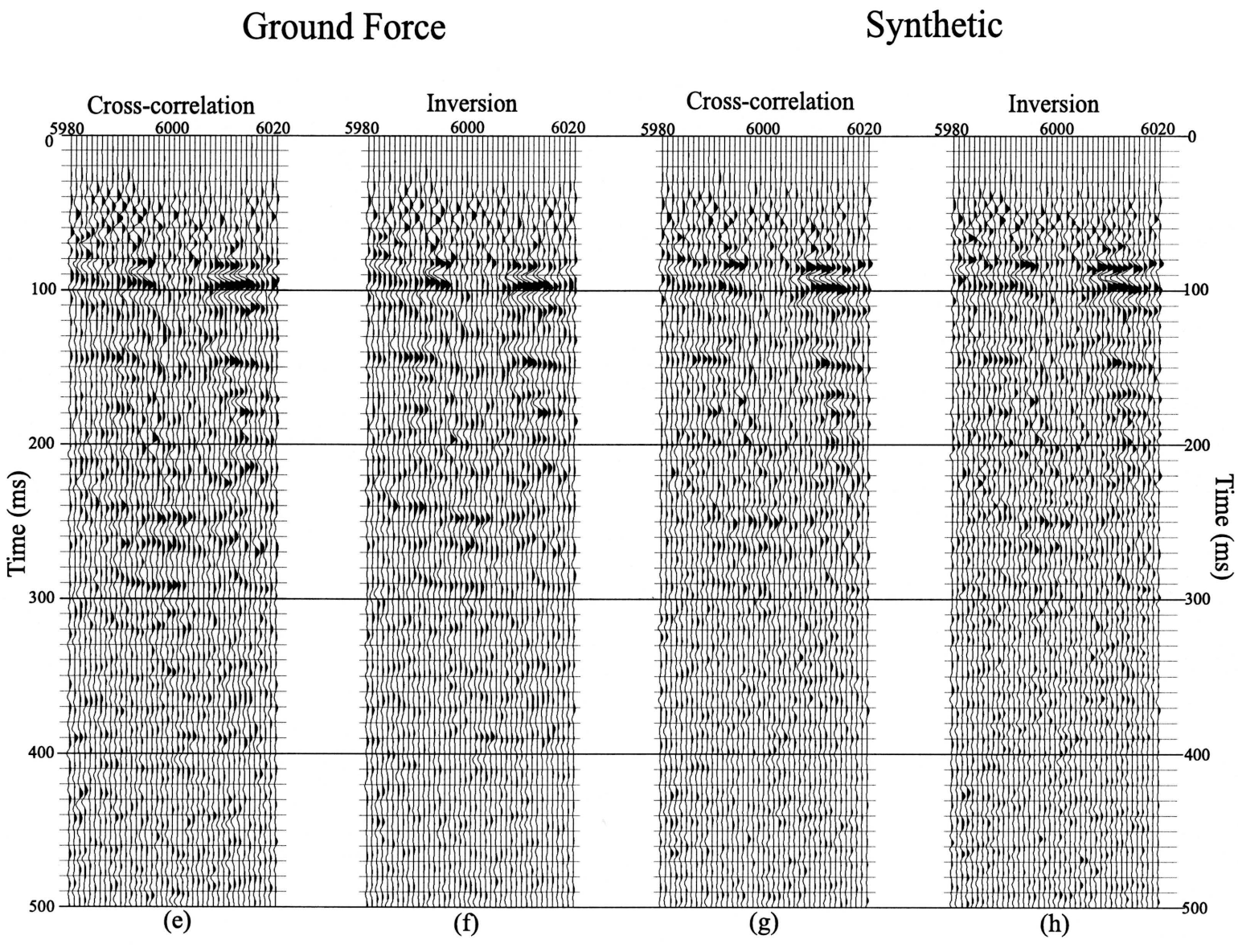
Ground Force
Synthetic
Cross-correlation
Inversion
Cross-correlation
Inversion
5980
6000
6020
0
100
200
300
400
500
Time (ms)
(e)
(f)
(g)
(h)

events to be migrated only fractions of a degree. Events of low dip are affected the least. Dips of less than 15 degrees are noted on the Zeandale seismic profile and thus the maximum dip change of reflecting events due to migration filtering is 0.03 degrees (Ivanov et al., 1998). After the migration filter was applied, it was necessary to apply automatic gain control (AGC) scaling with a window of 375 ms in order to see deeper events. The migration filter enhanced the entire seismic profile, but deeper reflections noted the most improvement (Fig 4.2).

5. Seismic Attributes

Dominant frequency of the Zeandale seismic line is 50 Hz (Fig. 5.1). Based on velocities obtained from a sonic log in a nearby well (Fig. 5.2), this represent a dominant wavelength of 37 m at 100 ms and 70 m at 550 ms. The resolution limits of this data are constrained by these wavelengths. Seismic data resolvability has been determined to be 1/20 of the dominant wavelength (Gochioco, 1991), ¼ of the dominant wavelength (Widess, 1973), and 1/3 of the dominant wavelength (Miller et al., 1995). However, these values represent the limits of resolution. As data become noisy or ringy, or both, the threshold of resolution is increased. To determine the true resolution of the Zeandale seismic data, at least two wells would have to be placed directly on the line to determine thicknesses of rock units along the profile and how these thicknesses change along the profile. Some estimation of the resolution can be made, though. Resolution of ½ the dominant wavelength has been suggested for noisy data (Widess, 1973) and if used for the Zeandale data yields a minimum bed resolution of 19.5m at 100 ms to 35 m at 550 ms. These values are assumed to be a reasonable estimate for the seismic data.

The basis for most of the geological correlations is a synthetic seismogram computed from well data and a Ricker wavelet (Fig. 5.3). The synthetic data were calculated from a sonic and density log acquired roughly 5 km (3 mi) east of the profile in section 26 of township 10 S, range 11 E. This was the closest sonic log to the survey. From sonic and density data, velocity and reflection coefficients were calculated. Finally, a Ricker wavelet of decreasing fundamental frequency (60-45Hz) was convolved with the reflection coefficient trace to yield the synthetic seismogram. A 50 Hz. Ricker wavelet displays very similar spectral characteristics to the spectrum of a stacked data trace (Fig. 5.1). The synthetic correlates reasonably well to the eastern end of the profile (Fig 5.4). This sonic log does not penetrate the basement, other nearby well data indicate a thickness of 60 m (200 ft) between the top of the Viola and the top of the Precambrian. Because this is nearly twice as large as the assumed minimum resolvable bed thickness at this depth, the triplet that correlates with the Viola reflection is interpreted to be the Viola limestone-Precambrian surface package of reflectors. Because collection of sonic data began at 77 m (255 ft), a static shift of about 70 ms was applied to the synthetic traces.

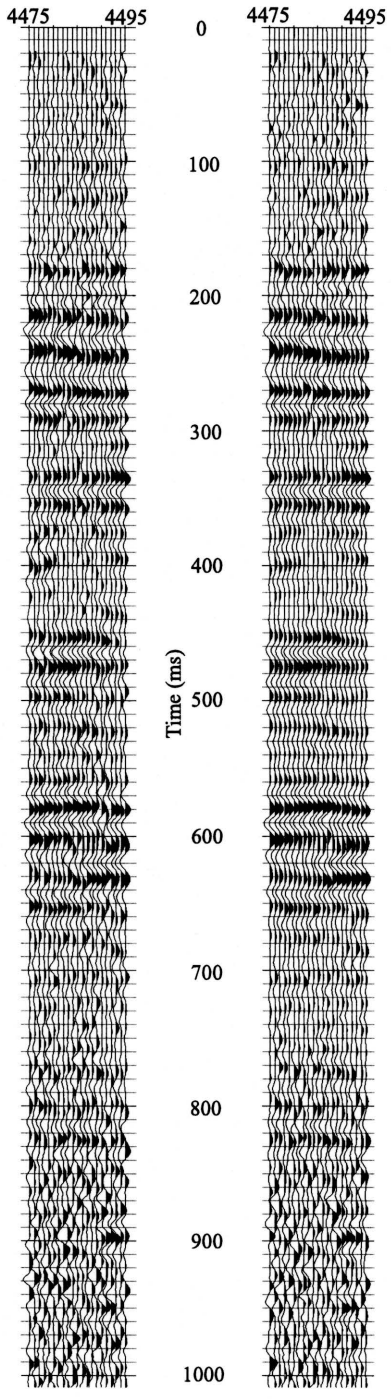

Figure 4.2 Comparison of stacked seismic data from the Forest City basin with and without migration filtering applied. Data without migration appear on the left and a migration filter has been applied to the data right. Horizontal axis represents CMP numbers.

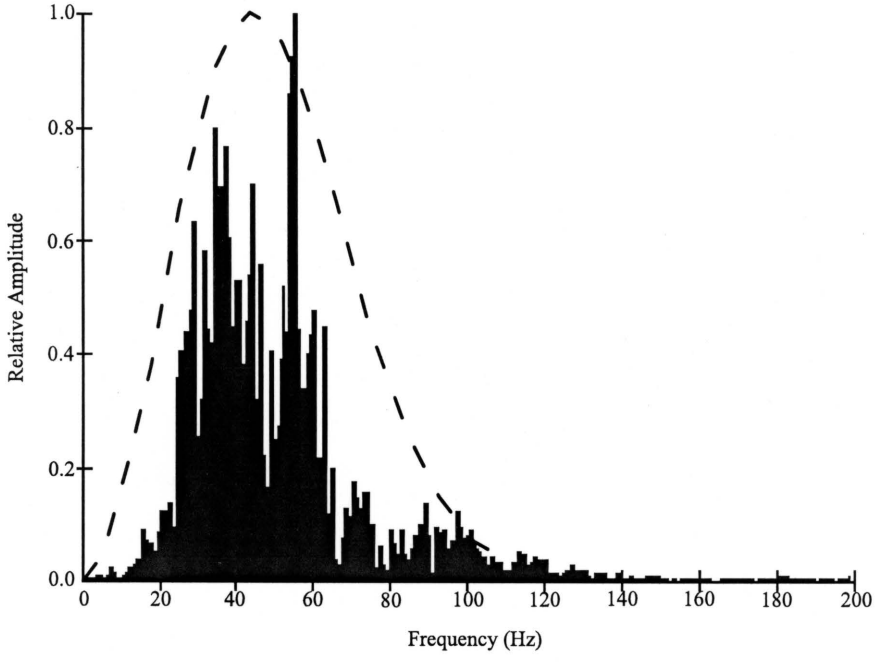

Figure 5.1 Spectrum of CMP 4800 stacked trace. Data trace occurs in the Forest City basin. Dominant frequency appears to be about 50 Hz. Dashed line outlines the spectrum of a 50 Hz Ricker wavelet.

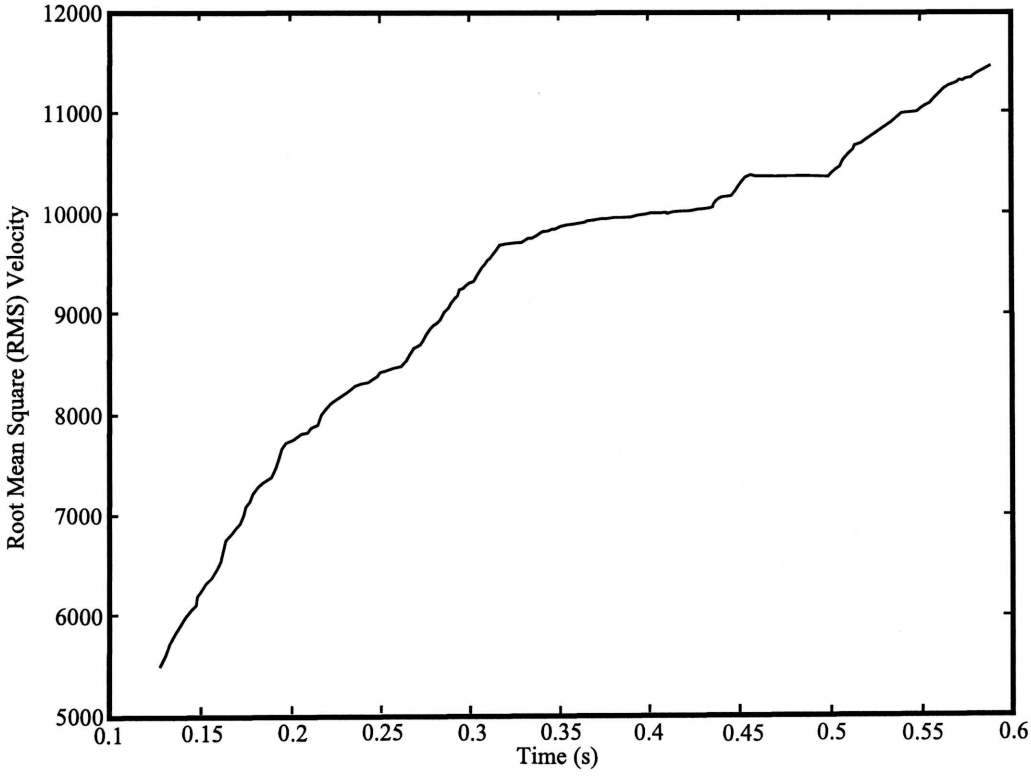

Figure 5.2 Time versus root mean square (RMS) velocity as calculated from the sonic log.

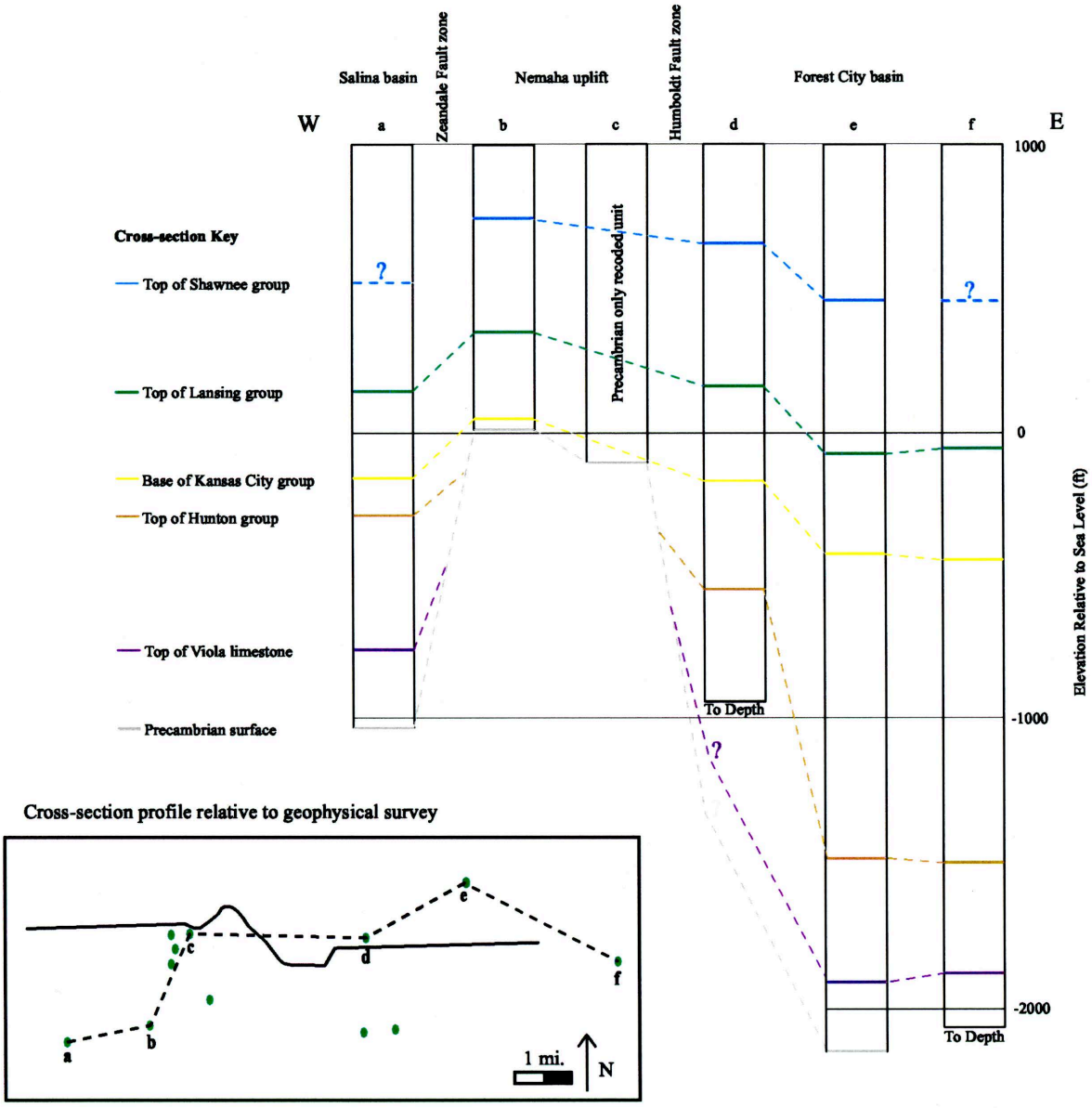

Figure 5.3 Cross-section of well data along the Zeandale profile. All tops are taken from completion cards. Inset map shows position of wells with respect to the profile. Lettered green dots are wells represented in the cross-section. Plain green dots are wells used to help in interpretation, but not represented on the cross-section.

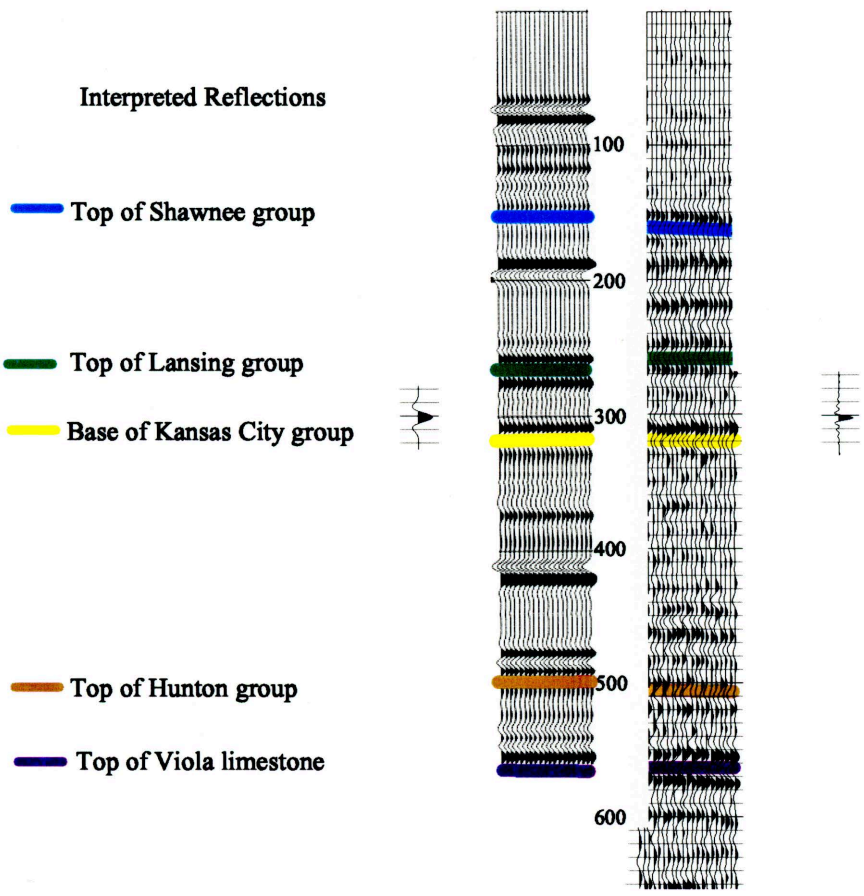

Figure 5.4 Comparison of the synthetic seismogram with a protion of the actual data. Vertical axis is time in milliseconds. Waveform at the far left is a 50 Hz ricker wavelet and represents the wavelet in the synthetic traces. Waveform at the far right is a Klauder wavelet produced from the autocorrelation of the synthetic vibrator sweep. Seismic traces on the left are the synthetic traces and seismic traces on the right are actual seismic data from the Forest City basin.

At around 870 ms in the Forest City basin, a seismic triplet occurs discontinuously. Utilizing a velocity of 3500 m/s (11500 ft/s), and 870 ms as a two-way traveltime, depth to this reflector is 1.5 km (5000 ft). Because 3500 m/s is the velocity at 550 ms, the RMS velocity at 870 ms is expected to be much greater than 3500 m/s so this value represents a minimum value and the calculated depth thus represents a minimum depth. Regardless, this value is much deeper than 900 m (3000 ft) at which drill data has confirmed granitic basement. When a hyperbola is fit to this event (Fig. 5.5), a velocity of 2400 m/s (8000 ft/s) results, much less than the expected value of >3500 m/s. The 2400 m/s velocity is expected at 290 ms. Because deep event seems to mimic the event at 290 ms (i.e. dips change along both events at similar locations) and has a very similar velocity, the 870 ms event is probably multiple of the 290 ms event, implying that there is also multiple energy at 580 ms, roughly at the location of the Viola. Because only a fraction of an acoustic waves energy is reflected at an interface and the multiple event has been reflected three times, it is likely much smaller in amplitude than the Viola reflection which has been reflected only once. An additional amount of the multiple energy is attenuated because it spends twice as long in the near surface materials than does the primary reflection. Thus, the Viola reflection is not obscured, but the added multiple energy may at a coincident time may contribute to degradation of the event.

6. Interpretations

The profile (Plates B & C) can is divided into five distinct parts from east to west: (1) the Forest City basin (CMP's 4000-4800), (2) the Humboldt fault zone (CMP's 4800-5100), (3) the Nemaha uplift (CMP's 5100-6420), (4) Zeandale Fault zone (CMP's 6420-6640), and (5) the Salina basin (CMP's 6640-7150).

6.1 Forest City basin

Seismic data in the Forest City basin (CMP's 4000-4800) suggest very little structure, undulation of only a few milliseconds, small scale faulting (CMP's 4450 and 4580), and one graben (CMP's 4520-4575) are apparent. The graben is also suggested by the gravity data. Pennsylvanian aged reflecting events appear lower amplitude and less continuous across the graben when compared to the same set of reflecting events just outside the graben (i.e. CMP's 4450-4490). All of the faulting is normal and appears to be related to structural disturbances in the basement. At least some of the offset has occurred in Pennsylvanian or later times because the three western faults have some expression in the Pennsylvanian sedimentary section.

6.2 Humboldt Fault zone

The Humboldt Fault zone (CMP 4800-5100) in the Paleozoic sedimentary rocks is a complex set of reverse and normal faults. The largest fault (CMP 5040) is a high angle west dipping reverse fault with 200 ms (1000 ft) of offset and occurs on the westernmost edge of the fault zone. This

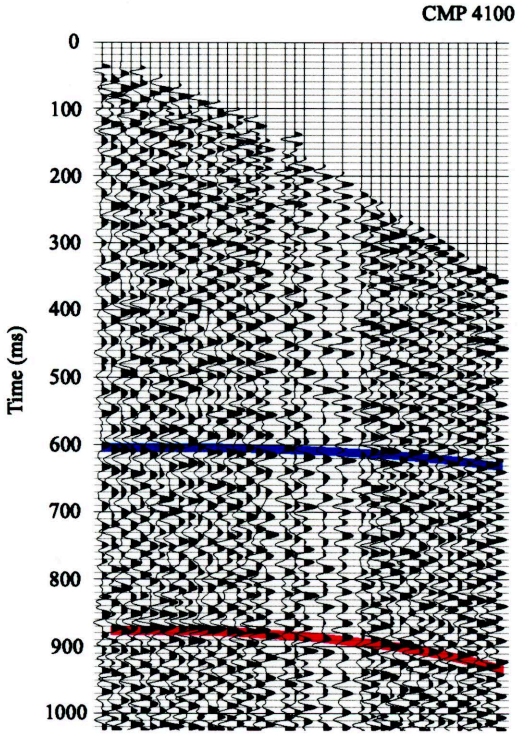

Figure 5.5 CMP gather from the Forest City basin. The reflection at 600 ms (blue line) is the Viola limestone and has a velocity of 3500 m/s. The event at 870 ms (red line) has a velovity of 2400 m/s, much slower than anticipated.

fault shows major movement before the deposition of the Kansas City group (Missourian Stage), and based on other published material occurred pre-Desmoinian (i.e. Merriam, 1963). Some offset and folding is present in the Pennsylvanian sedimentary strata, but this is minor relative to the pre-Missourian movement. One other sizable (200 ft) reverse fault is noted at CMP 4900, but this fault dips to the east. This fault shows a reverse sense of movement in pre-Missourian sediments. However, this same fault has a normal sense of movement in the overlying Pennsylvanian sedimentary rocks. For this to occur the reverse faulting must have occurred prior to deposition of the Pennsylvanian sediments. Then after the deposition of the Pennsylvanian sediments, the fault was reactivated, but with a normal sense of movement. This normal slip was much less than the reverse slip or the fault would appear to be a normal fault throughout the section retaining no record of the reverse slip. Slightly to the east of the reverse faulting (CMP 4920–4800) several normal faults of small throw are present. Not all of these faults penetrate the Pennsylvanian sediments, however several do (i.e. CMP 4830, 4875). Individual normal faults appear to have constant throw. This suggests that all of the normal faulting has taken place after the deposition of Shawnee Group sediments, or post-Missourian. It is probable that these normal faults occur along joints or reverse faults of small throw set up in the compressional stress field of the main phase of reverse faulting. At a later time, the stress field became extensional and the normal faulting took place (Fig. 6.1).

6.3 Nemaha uplift

The Nemaha uplift portion of the profile (CMP's 5100-6420) is a reasonably flat feature that extends 11 km (7 mi) across the profile. The Kansas City group lies directly on the Precambrian granite along the length of the uplift since pre-Pennsylvanian sediments have been eroded or not deposited. The reflections present on the Nemaha uplift from the Shawnee group to the base of the Kansas City show excellent correlation to the same package of reflections in the Forest City basin (Fig. 6.2) and this correlation aided in the interpretation of the Nemaha ridge. Across the length of the profile, several small faults and grabens occur with fault offsets on the order of 15-30 m (50-100 ft). It is impossible to interpret if any of the movement of the faults along the length of the uplift took place pre-Pennsylvanian because pre-Pennsylvanian sediments are not present. All interpreted faulting along the length of the uplift is normal, suggesting an extensional regime at the time of faulting.

6.4 Zeandale Fault zone

The western edge of the uplift (CMP 6420-6620) is defined by another fault zone that will be referred to as the Zeandale Fault zone. This fault zone represents the boundary of the Nemaha uplift and the Salina basin. This structure appears to be much simpler than the Humboldt Fault zone, and all interpreted faulting in this zone is normal. The majority of fault displacement in the

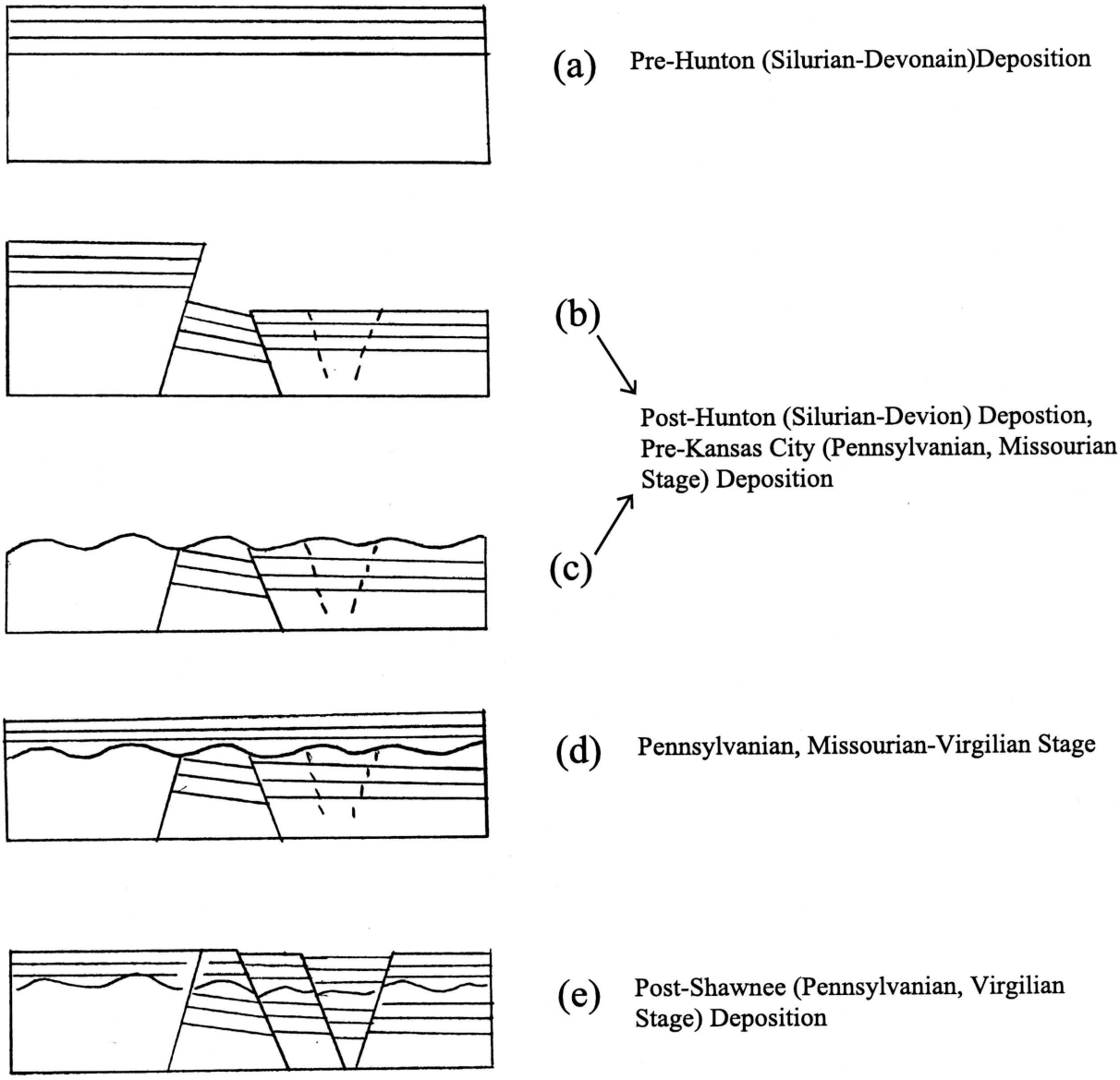

Figure 6.1 Cartoon schematic of sequence of events that produced the Humboldt Fault zone. In pre-Mississippian time (a) sediments are deposited on top of Precambrain granitc basement. Faulting (b) and erosion(c) occur post-Hunto deposition, pre-Kansas City deposition (Upper Devonian - Middle Pennsylvanian). This faulting is reverse and thus in a compressional stress regime. Deposition of Pennsylvanian aged sediments then takes place (d). Finally, normal faults form (e) after the deposition of Shawnee sediments (Virgilian stage). Because at least one reverse fault shows a reversal of throw in Penssylvanian aged sediments, it is possible that many of these normal faults may have formed along existing joints or reverse faults of small throw the formed during (b). This may show a change in the stress field from compressional to extensional, or simply a relaxation of the prior compressional stresses.

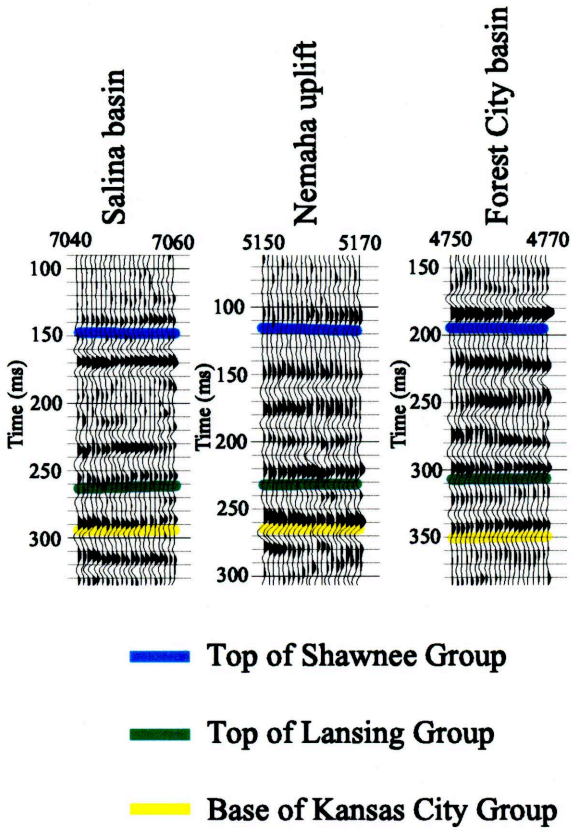

Figure 6.2 Comparion of reflection character of Pennsylvanian sedimentary section across the Zeandale seismic line.

Zeandale Fault zone is interpreted to have occurred pre-Pennsylvanian because only one of the faults penetrates the Pennsylvanian aged sediments over this Zeandale Fault zone. Folding is noted in the Pennsylvanian sediments that could account for the displacement across the four western faults in this zone (CMP's 6550-6640). However, because of the occurrence of a wedge Hunton group rocks (CMP's 6570-6640) that is either onlapping or truncated, some uplift had to have occurred pre-Pennsylvanian (Fig. 6.3 & 6.4). For instance, if the rocks are onlapping, then CMP's 6570-6640 must have been a positive feature during the time of deposition. If the rocks are eroded, then they must have been exposed prior to the deposition of the Pennsylvanian sedimentary rocks. A graben with large throw on the bounding faults is present at CMP 6430-6520. There are no coherent events above Viola triplet and beneath the Pennsylvanian sediments (280-360 ms) so it is impossible to say with confidence what type of sediment package makes up this area. Since the base of the Kansas City group is not traceable across this graben at least some of the movement probably occurred in upper Pennsylvanian time.

6.5 Salina basin

The package of Mississippian sediments that is present in the Forest City basin is absent in the Salina basin side of the profile (Merriam, 1963). The pre-and post-Mississippian sedimentary rock columns are very similar in lithology and thicknesses based on well data. Reflections from the Hunton group through the Viola limestone in the Salina basin possess remarkable similarity to the same package of reflections in the Forest City basin (Fig. 6.5). The Shawnee group through the base of the Kansas City group can also be correlated directly with high confidence across the uplift (Fig. 6.2). These observations were used to help guide larger scale interpretations.

The Salina basin (CMP's 6640-7150) shows little structure in post Ordovician sedimentary rocks other than one graben occurs at CMP's 6990 – 7030. This graben is normally faulted and the bounding faults appear to be of small (< 20 m) throw. A sizeable set of normal faults (CMP's 7050-7120) that penetrate only pre-Hunton sedimentary rocks have been interpreted at the far west end of the line. Timing of this activity is thus constrained to upper Ordovician to Silurian (post-Viola, Pre-Hunton). Little confidence may be had in this interpretation because no previous studies have suggested large amounts of offset (> 200 m) pre-Hunton deposition and post-Viola limestone deposition. No drill data exists to confirm this interpretation. It is also suspect that this event occurs at the end of the line where fold becomes increasingly low. It has been offered only to suggest a further area of study.

7. Conclusions

This study successfully defined the character and structural complexity of the Humboldt fault zone/Nemaha uplift system within the Paleozoic sedimentary rocks in northern Wabaunsee county and southern Riley county. In the place the seismic profile crosses the Humboldt Fault zone the

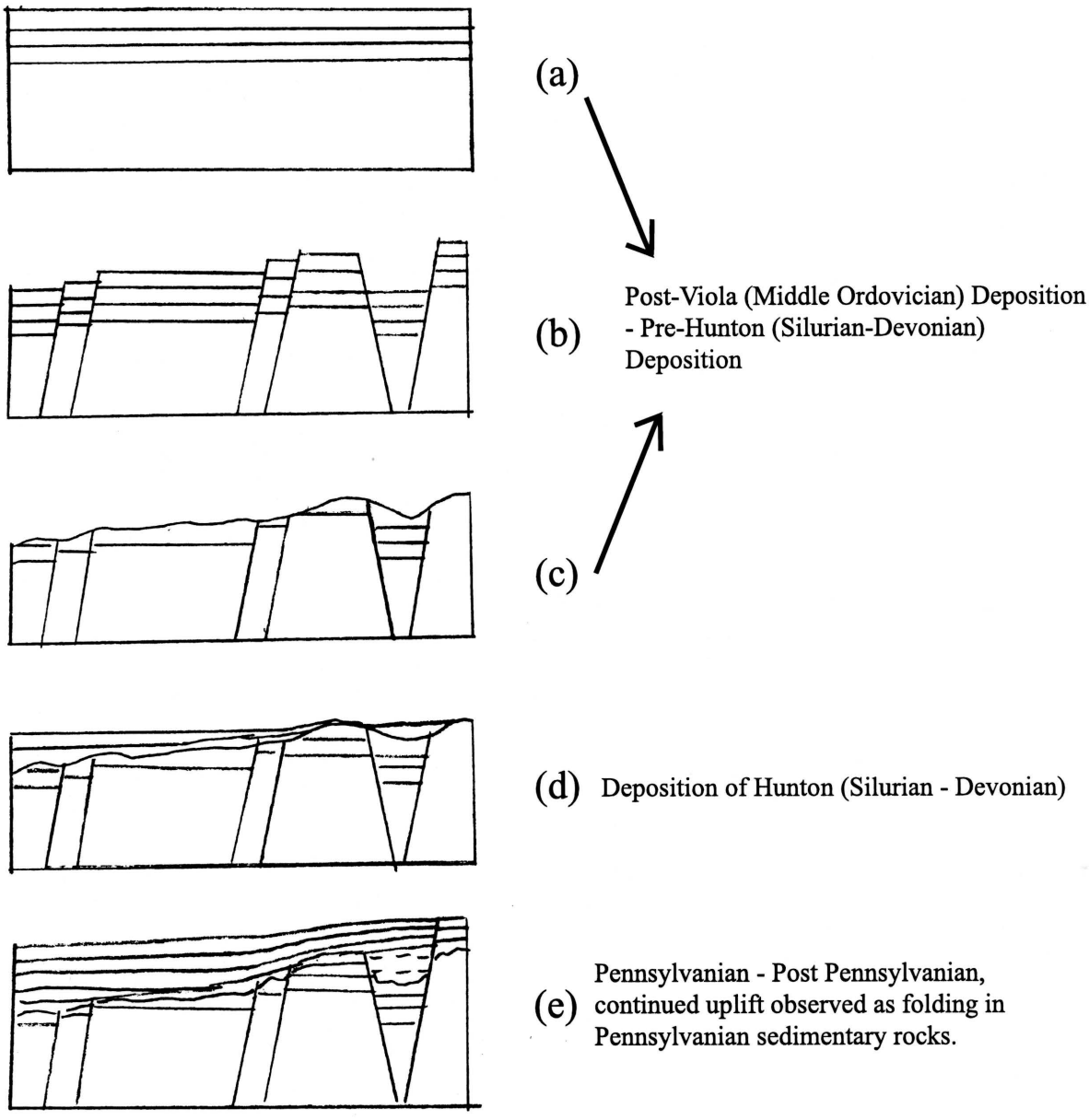

Figure 6.3 Cartoon schematic of one possible sequence of events that produced the Zeandale Fault zone and faulting imaged in the Salina basin. Post Viola deposition and pre-Hunto deposition, noraml faulting occurs, followed by erosion (a-c). Hunton group sedimentary rocks are deposited, onlapping the Nemaha uplift (d). Finally, Pennsylvanian aged sedimentary rocks are deposited (e). Some uplift is noted post-Pennsylvanian because of the folding noted in the Pennsylvanian aged sedimentary rocks.

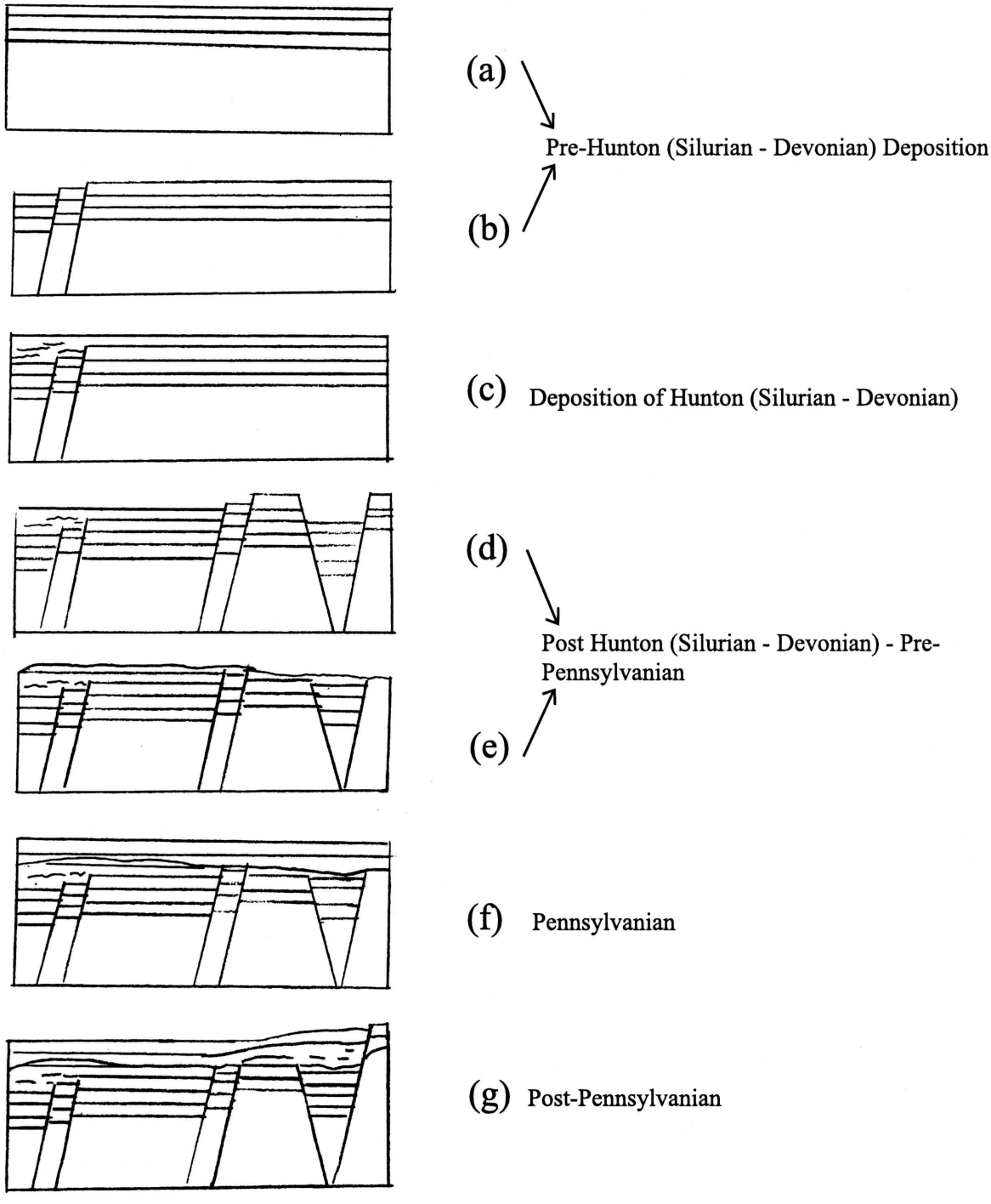

Figure 6.4 Cartoon schematic of second possible sequence of events that produced the Zeandale fault zone and faulting imaged in the Salina basin. Faulting in the Salina basin occurs post-Viola deposition, pre-Hunton deopsition(a-b). In Silurian-Devonain time, Hunton group rocks are deposited (c). Faulting of the Zeandale Fault zone followed by erosion occurs post-Hunton deposition, pre-Pennsylvanian (d-e). Pennsylvanian sedimentary rocks are deposited (f). Someuplift is noted pst-Pennsylvanian because of the folding noted in the Pennsylvanian aged sedimentary rocks.

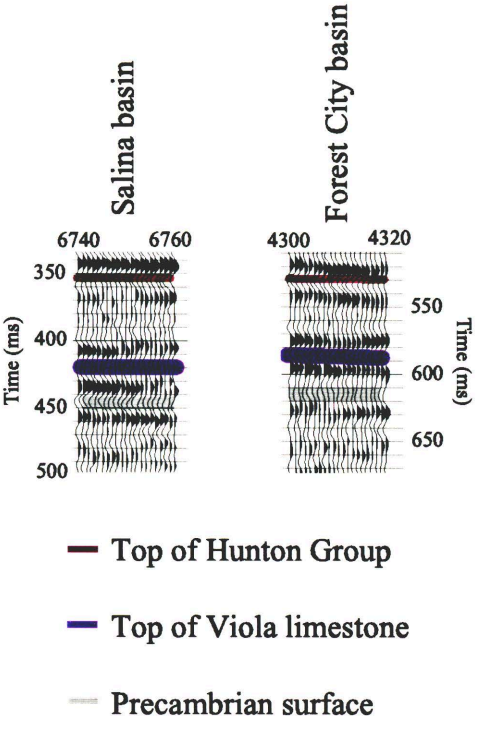

Figure 6.3 Comparison of reflection characeter of pre-Mississippian sediments across the Zeandale seismic line. These rocks are absent on the Nemaha uplift.

Paleozoic sedimentary rocks can be characterized as a complex set of reverse and normal faults with a cumulative offset of over 600 m (2000 ft). Two episodes of faulting are evident. The first phase of faulting occurred pre-Desmoinesian and produced reverse faulting with large fault offsets. The fault with the largest apparent offset (CMP 5040) was formed during this phase and has 300 m (1000 ft) of apparent displacement based on the seismic data. After the deposition of the Shawnee Group (Virgilian stage), the stress field shifted into an extensional regime. Because at least one fault in the fault zone shows a reversal of displacement (CMP 4900), the formation of normal faults probably took place along existing small faults and joints that formed during the earlier phase of faulting. Because observed offsets in the normal faults are relatively small (less then 50 m), it is possible this normal phase of faulting was a relaxation of the compressional field (Gay, 1999).

Two other seismic studies of the Humboldt fault in Northeastern Kansas have been published. One in northern Nemaha county showed a single normally dipping fault (Stander, 1981; Stander 1989). Because this seismic data did not image sedimentary rocks older than Cherokee group (Pennsylvanian, Desmoinian stage) the observed normal faulting is consistent with the interpretation offered in this paper. It is possible that if deeper sedimentary rocks had been imaged a reverse faulting would have been noted. The other in central Nemaha county shows a multitude of faulting, including one fault interpreted by the author as "a near vertical fault … [that] suggests reverse faulting." It is finally stated that any interpretation of this fault other than vertical of reverse would be difficult (Steeples, 1982; Steeples, 1989). Furthermore, it might be possible to reinterpret some of the normal faults as reverse faults such that any differences between this data set and the Zeandale line are resolved.

The Zeandale Fault zone occurs on the western edge of the Nemaha uplift. This fault zone is a complex set of normal faults with over 300 m (1000 ft) of cumulative displacement. Most of the faulting has expression that is limited to pre-Pennsylvanian sediments on the seismic data. However, a couple of the interpreted faults seem to extend into the overlying Pennsylvanian sediments but with much smaller throws than observed from the faulting evident in the deeper sediments. Because of the onlap/truncation of Hunton sedimentary rocks at CMP 6600, the majority of the uplift occurring on this fault zone is interpreted to be pre-Pennsylvanian, but the small scale faulting and gently folding of Pennsylvanian sedimentary rocks suggests a second period of movement post-Shawnee.

Interpretation of the potential field data is not as detailed as hoped. What originally had been thought to be faults in this potential field data do not seem to match the seismic data. For the gravity data this may simply be due to a low density contrast (0.2 g/cm^3) between the Paleozoic section and the Precambrian granite. As can be seen in (Fig. 7.1), Pennsylvanian aged and

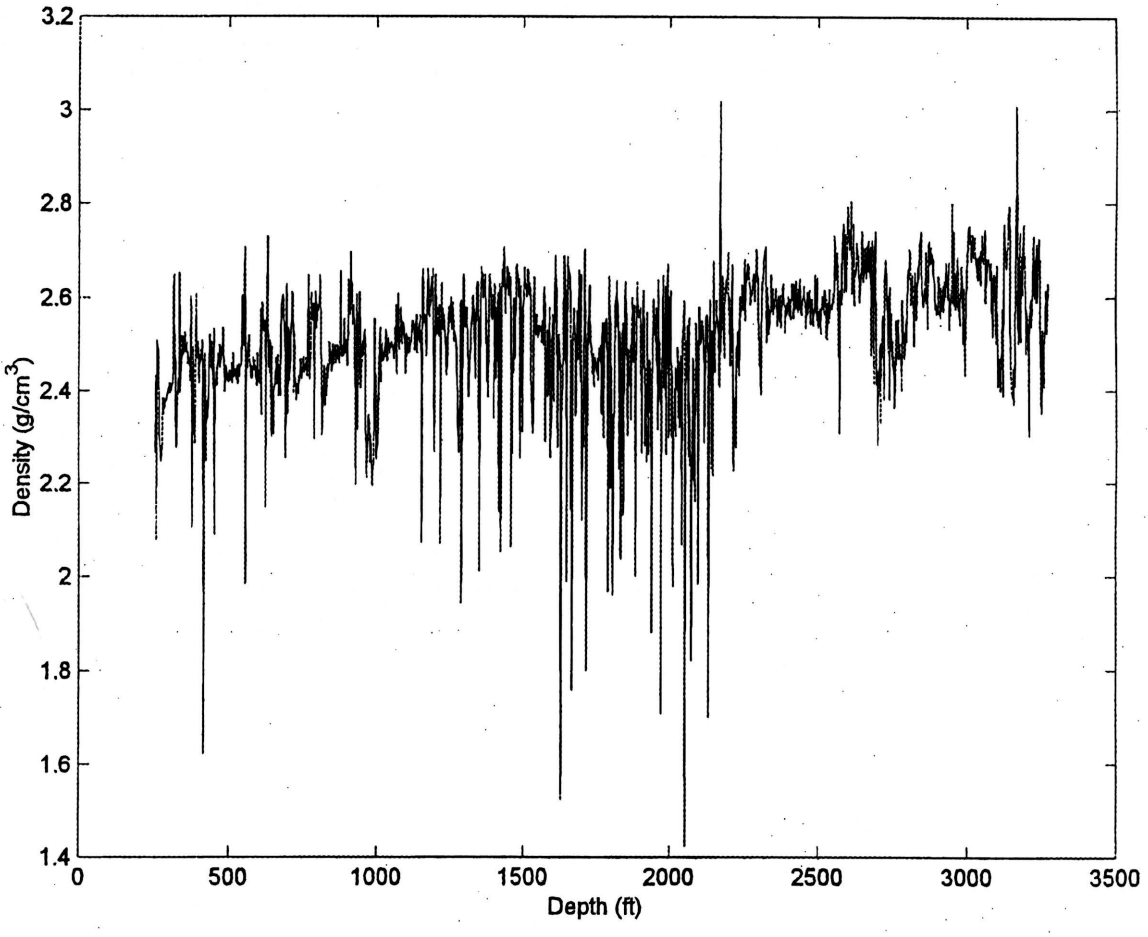

Figure 7.1 Density log from the same well that the sonic log was aquired at. Note the change in average density occuring at about 2100 feet.

younger rocks have an average density of 2.4-2.5 g/cm^3 and pre-Pennsylvanian sedimentary rocks have an average density of 2.6 g/cm^3. Xia and Sprowl (1995) report an average crustal density in Kansas of 2.63 g/cm^3, and Xia (1992) reports a value of 2.67 g/cm^3. Because of this low-density contrast, small-scale features simply are not resolved.

A magnetic data low at mile 8.9, CMP 5500 (Fig. 3.5 & 3.13) does not correspond to any major change in depth to basement. A small graben has been interpreted on the seismic data from this region, but nothing is evident that would explain low of this magnitude. The magnetic data are either being influenced by deeper bodies, or changes in the internal magnetic susceptibility of the granite are present. Neither possibility can be confirmed or refuted without physical sampling.

Potential field data acquired on 0.16 km (0.1 mi) spacing do not appear to be sufficient to map small scale (15-30 m) faulting in this region. The Humboldt fault zone/Nemaha uplift system are mappable using potential field methods, especially when residuals are calculated, but larger station spacing (1 km) would probably be sufficient, and data near this scale (1.6 X 1.6 km) already exist (Xia et. al., 1995). It may be possible that potential field data collected on a grid with tight spacing would show a better correlation with seismic data after residuals are calculated. This is essentially the method suggested by Gay (1995) to map basement in Kansas.

By plotting the location of the Humboldt Fault zone on a topographic map (Plate D), a definite relation between the fault zone and a change in surficial topography is apparent, from hilly terrain on the eastern side into Kansas river valley sediments on the western side. The bedrock also changes near this point from Pennsylvania aged rocks east of the fault zone to Permian aged sedimentary rocks of the west side of the fault zone, though the exact contact is obscured by the river sediments (Mudge and Burton, 1959). A northwesterly linear trend is apparent for several miles to the north along the river sediment/Pennsylvanian aged rock contact, and also be can traced in the course of the Kansas river (Plate D) (U.S.G.S. , 1990). This trend probably represents the strike of the Humboldt fault zone.

It is not possible with one two-dimensional seismic profile to determine strike of fault planes or much oblique character exists in the faults. Some oblique character is expected if the Humboldt fault zone/Nemaha uplift system is a wrench system, some oblique character is to be expected. These data neither confirm nor deny that hypothesis. A few kilometer square 3-D survey over the Humboldt Fault zone would help to delineate the strike of the fault zone and any horizontal or rotational motion is present in the fault zone.

References

Agocs, W.B., 1959. Airborne Magnetometer Profiles, Morris and Wabaunsee Counties, Kansas: *in* Hambelton, W.W., (ed.), Symposium on Geophysics in Kansas, Bulletin 137: Kansas Geological Survey, Lawrence, Kansas, p. 175-180.

Allen, K.P., Johnson, M.L., and May, J.S., 1998. High Fidelity Vibratory Seismic (HFVS) Method for Acquiring Seismic Data: *in* SEG Abstracts, 68th Annual Meeting, v. 1., p. 140-143.

Baars, D.L., 1995. Basement Tectonic Configuration in Kansas: *in* Anderson, N.L., and Hedke, D.E., (eds.), Geophysical Atlas of Selected Oil and Gas Fields in Kansas, Bulletin 237: Kansas Geological Survey, p. 7-9.

Baars, D.L., and Maples, C.G., 1998. Lexicon of Geological Names of Kansas (through 1995), Bulletin 231: Kansas Geological Survey, Lawrence, Kansas. 271 p.

Baysinger, B.L. 1963. A Magnetic Investigation of the Nemaha Anticline in Wabunsee, Geary, and Riley Counties, Kansas: Master's Thesis, Kansas State University, Manhattan, Kansas. 46 p.

Berendsen, P., and Blair, K.P., 1986. Subsurface structural map over the Central North American rift system (CNARS), central Kansas, with discussion: Subsurface Geology Series 8, Kansas Geological Survey, Lawrence, Kansas. 16 p. , 7 maps.

Berendsen, P. and Blair, K.P., 1995. Structural Development of the Nemaha Tectonic Zone in Kansas, *in* Johnson, K.S. (ed.), Structural styles in the southern Midcontinent, 1995 symposium: Oklahoma Geological Survey Circular 97, p. 208-214.

Berendsen, P., and Blair, K.P., 1996. Structural Configuration of the Precambrian Basement, Kansas. Map M-45: 1: Kansas Geological Survey, Lawrence, Kansas.

Berendsen, P., and Blair, K.P., 1996. Precambrian Subcrop, Kansas. Map M-45: 2: Kansas Geological Survey, Lawrence, Kansas.

Berendsen, P., and Blair, K., 1996. Midcontinent Rift System in Kansas. Text to accompany maps M-45:1&2: Kansas Geological Survey, Lawrence, Kansas. 4 p.

Berendsen, P., Doveton, J., Gerhard, L., Newell, K.D., Steeples, D., Watney, W.L., and Borcherding, R., 1988. Preliminary geologic report of the Texaco 1 Poersch borehole. Oil and Gas Journal, Oct. 31, p. 48-54.

Burger, H.R., 1992. Exploration Geophysics of the Shallow Subsurface. Perntice Hall, Englewood Cliffs, New Jersey. 489 p.

Cannon, W.F., Green A.G., Hutchinson, M.L., Bernd, M., Behrendt, J.C., Halls, H.C., Green, J.C., Dickas, A.B., Morey, G.B., Sutcliffe, R., and Spencer, C., 1989. The North American Midcontinent Rift Beneath Lake Superior From GLIMPCE Seismic Reflection Profiling: Tectonics, v. 8, no. 2, p. 305-332.

Chun, J.H., and Jacewitz, C.A., 1981. Fundamentals of frequency domain migration: Geophysics, v. 46, p. 717-733.

Cole, V.B., 1975. Subsurface Ordovician-Cambrian Rocks in Kansas: Subsurface Geology Series 2, Kansas Geological Survey, Lawrence, Kansas. 18 p.

Cole, V.B., 1976. Configuration of the tops of Precambrian rocks in Kansas, map M-7: Kansas Geological Survey, Lawrence, Kansas.

Cole, V.B., and Watney, W.L., 1985. List of Kansas wells drilled into Precambrian rocks: Subsurface Geology Series 7, Kansas Geological Survey, Lawrence, Kansas. 139 p.

Dubois, S.M., 1978. The origin of surface lineaments in Nemaha County, Kansas: Master's Thesis, The University of Kansas. 37 p.

Gay, S.P., 1995. Basement Control of Selected Oil and Gas Fields in Kansas as Determined by Detailed Residual Aeromagnetic Data: *in* Anderson, N.L., and Hedke, D.E., (eds.), Geophysical Atlas of Selected Oil and Gas Fields in Kansas, Bulletin 237: Kansas Geological Survey, p. 10-16.

Gay, S.P., 1999. Strike-slip compressional thrust-fold nature of the Nemaha system in Eastern Kansas and Oklahoma; *in* Merriam, D.F., Transactions of the 1999 AAPG Midcontinent Section Meeting, Kansas Geological Open file report 99-28, p. 39-49.

Geyer, R.L., 1969. The Vibroseis® system of seismic mapping: Journal of the Canadian Society of Exploration Geophysicists, v. 6, p. 39-58.

Gochioco, L.M., 1991. Tuning effect and interference reflections from thin beds and coal seams: Geophysics, v. 56, no. 8, p. 1288-1295.

Harding, T.P., 1983. Divergent wrench fault and negative flower structure, Andaman Sea: *in* Bally, A.W. (ed.), Seismic expression of structural styles, Studies in geology series #15, V. 3; The American Association of Petroleum Geologists. Tulsa, Oklahoma. p. 4.2-1.

Ivanov, J., Miller, R.D., and Xia, J., 1998. High frequency random noise attenuation on shallow seismic reflection data by migration filtering: *in* SEG Abstracts, 68th Annual Meeting, v. 1., p. 870-873.

Konig, M., 1971. A Magnetic Profile Across the Nemaha Anticline in Pottawatomie and Western Jackson Counties, Kansas: Master's Thesis, Kansas State University, Manhattan, Kansas. 87 p.

Lee, W., 1943. The Stratigraphy and Structural Development of the Forest City Basin in Kansas, Bulletin 51: Kansas Geological Survey, Lawrence, Kansas. 142 p.

Lee, W., 1956. Stratigraphy and Structural Development of the Salina Basin Area, Bulltin 121: Kansas Geological Survey, Lawrence, Kansas. 167 p.

Lyons, P.L., 1959. The Greenleaf Anomaly, a Significant Gravity Feature: *in* Hambelton, W.W., (ed.), Symposium on Geophysics in Kansas, Bulletin 137: Kansas Geological Survey, Lawrence, Kansas, p. 105-120.

Merriam, D.F., 1963. The Geologic History of Kansas, Bulletin 162: Kansas Geological Survey, Lawrence, Kansas, 317 p.

Miller, R.D., Anderson, N.L., Feldman, H.R., and Franseen, E.K., 1995. Vertical resolution of a seismic survey in stratigraphic sequences less than 100 m deep in southeastern Kansas: Geophysics, v. 60, no. 2, p. 423-430.

Mudge, M.R., and Burton, R.H., 1959. Geology of Wabaunsee County, Kansas. United States Geological Survey Bulletin 1068, 210 p.

Newell, K.D., 1995. Overview of Petroleum Geology and Production in Kansas: *in* Anderson, N.L., and Hedke, D.E., (eds.), Geophysical Atlas of Selected Oil and Gas Fields in Kansas, Bulletin 237: Kansas Geological Survey, p. 2-6.

Serpa, L., Setzer, T., and Brown, L., 1989. COCORP seismic-reflection profiling in northeastern Kansas: *in* Steeples, D.W. (ed.), Geophysics in Kansas, Bulletin 226: Kansas Geological Survey, Lawrence, Kansas, p. 165-176.

Serpa, L., Setzer, T., Farmer, H., Brown, L., Oliver, J., Kaufman, S., Sharp, J., and Steeples, D.W., 1984. Structure of the Keweenawan Rift from COCORP Surveys Across the Midcontinent Geophysical Anomaly in Northeastern Kansas: Tectonics, v. 3, no. 3, p.367-384.

Sharma, P.V., 1986. Geophysical Methods in Geology, 2nd Edition. Elsevier, New York. 442 p.

Smith, J.G., and Jenkersen, M.R., 1998. Aquiring and processing marine vibrator data in the transition zone: *in* SEG Abstracts, 68th Annual Meeting, v. 1., p. 136-139.

Somanas, C. Knapp, R.W., Yarger, H.L., and Steeples, D.W., 1989. Geophysical model of the Midcontinent Geophysical Anomaly in northeastern Kansas: *in* Steeples, D.W. (ed.), Geophysics in Kansas, Bulletin 226: Kansas Geological Survey, Lawrence, Kansas, p 215-228.

Stander, T.W., 1981. Structural Nature of the Humboldt Fault zone in Northeastern Nemaha County, Kansas: Master's Thesis, The University of Kansas, Lawrence, Kansas. 23 p.

Stander, T.W., 1989. Structural nature of the Humboldt Fault zone in northeastern Nemaha County, Kansas: *in* Steeples, D.W. (ed.), Geophysics in Kansas, Bulletin 226: Kansas Geological Survey, Lawrence, Kansas, p. 117-128

Steeples, D.W., 1989. Structure of the Salina-Forest City interbasin boundary from seismic studies: *in* Steeples, D.W. (ed.), Geophysics in Kansas, Bulletin 226: Kansas Geological Survey, Lawrence, Kansas, p. 31-52.

Widess, M.B., 1973. How thin is a thin bed?: Geophysics, v. 38, no. 6, p. 1176-1180.

Wilcox, R.E., Harding, T.P., Seely, D.R., 1973. Basic Wrench Tectonics: The American Association of Petroleum Geologists Bulletin, v. 57, no. 1, p. 74-96.

Woelck, T.S., and Hinze, W.J., 1991. Model of the midcontinent rift system in northeastern Kansas: Geology, v. 19, p. 277-280.

Woelck, T.S., and Hinze, W.J., 1995. Midcontinent rift system in Northeastern Kansas: *in* Anderson, N.L., and Hedke, D.E., (eds.), Geophysical Atlas of Selected Oil and Gas Fields in Kansas, Bulletin 237: Kansas Geological Survey, p. 22-27.

Xia, J., 1992. Three-dimensional inversion of potential field data with application to Kansas; Ph.D. dissertation, the University of Kansas, Lawrence, Kansas. 132 p.

Xia, J., and Miller, R., 1997. Hum filter: power line noise eliminator: 1997 SAGEEP Meeting at Chicago, Illinois.

Xia, J., Miller, R.D., and Steeples, D.W., 1995. Aeromagnetic map of Kansas, reduced to the pole with second vertical derivative calculated: Kansas Geological Survey Map series, M 41-A. Kansas Geological Survey, Lawrence, Kansas.

Xia, J., Miller, R.D., and Steeples, D.W., 1995. Bouguer gravity map of Kansas, second vertical derivative caluclated: Kansas Geological Survey Map series, M 41-B. Kansas Geological Survey, Lawrence, Kansas.

Xia, J., and Sprowl, D.R., 1995. Moho depths from gravity inversion assuming exponential density contrast: Computers and Geosciences, v. 21, no. 2, p. 237-244.

Yilmaz, O., 1987. Seismic data processing: Society of Exploration Geophysicists, Tulsa, Oklahoma. 526 p.

Zeller, D.E. 1968. The stratigraphic succession in Kansas: Kansas Geological Survey, Bulletin 189. Kansas Geological Survey, Lawrence, Kansas. 81 p.

Appendix A

The following equations were taken primarily from Burger (1992) and Sharma (1986).

After corrections were applied to the data, maximum error was calculated for each data set. Error in the gravity data was calculated in the following manner. As stated in section 3, the maximum elevation error was assumed to be 1.5 m. This value affects both the free-air and Bouguer corrections. An equation representing the free air correction is:

$$FA_g = (0.3086 + 0.00023\cos 2\phi - 0.00000002z)z \ mGal$$

$$z = meters \ from \ datum \ elevation(positive \ if \ greater \ than \ datum)$$

$$\phi = latitude$$

Because the last two terms are very small, the value for the free air correction is essentially 0.3086 mGal/m. The Bouguer correction is given by the following equation:

$$B_g = (-0.04193\rho \ z) \ mGal$$

$$z = meters \ from \ datum \ elevation(positive \ if \ greater \ than \ datum)$$

$$\rho = density \ of \ rock \ (g/cm^3)$$

Density was assumed to be 2.67 g/cm^3. Variations from this value for the density were not figured into the error. This value has been shown to be a valid density to use in Kansas (e.g. Xia, 1992). Thus, the total elevation correction applied to this data may be represented by:

$$E_g = FA_g - B_g$$

$$E_g = (0.3086 - 0.04193\rho)z \ mGal$$

Utilizing $\pm$ 0.762 m, the total error associated with the elevation corrections is thus $\pm$0.1498 mGal. Correction for a shift in latitude is given by the following equation:

$$C_\phi = (0.812\sin 2\phi \ )y_{km} \ mGal$$

$$\phi = latitude \ of \ base \ station$$

$$y_{km} = kilometers \ north \ or \ south \ of \ base \ station(positive \ indicates \ south \ of \ base \ station)$$

or, in meters:

$$C_\phi = (0.000812\sin 2\phi \ )y_m \ mGal$$

$$y_m = same \ as \ y_{km} \ above \ but \ in \ meters$$

For the base station used in this survey, ϕ=0.6832818, in radians. This value was taken from the topographic map. Because all values are relative to this base station, very large variations in phi will have little effect on the final latitude correction value. If this phi value is varied by a full degree, the C_ϕ varies by only 0.00053 mGal/km. Certainly the base station is locatable to much less than a degree (probably to within minutes or even seconds), thus the phi value was considered to have no noticeable error associated with it. Using the above value for phi, the correction is:

$$C_\phi = .795y_{km} \ mGal$$

Again, y_{km} should be positive if the reading was south of the base station, and negative if the reading was north of the base station. I assumed that each station was locatable to within $\pm$ 0.1 cm on the topographic map. The topographic maps used were all 1:24000 scale, so $\pm$ 0.1 cm error on the map translates into $\pm$ 24 m of error associated with each latitude reading. This value was used to estimate the latitude correction error, which is thus $\pm$ 0.019 mGal.

As an estimation of the drift error, it was assumed that the absolute difference between the base station readings represented the error. In other words, if one base station reading was A_g, and the next base station reading was B_g, the error associated with this data collected in the time in-between the collection of A_g and B_g, is the absolute value of A_g-B_g.

The gravity survey has three sources of error associated with it. They are:

σ_E = *Error associated with elevation estimation.*

σ_L = *Error associated with latitude estimation.*

σ_D = *Error associated with drift correction estimation*

The total error was calculated as a RMS error, and is given by the following equation:

$$\sigma_{TOTAL} = \sqrt{\sigma_E^2 + \sigma_L^2 + \sigma_D^2} \ .$$